

**Optimization of a powder-based solid dosage form
of TNF- α siRNA-loaded lipidoid-polymer hybrid
nanoparticles designed for pulmonary delivery**

Laure Harinck

A Master dissertation for the study programme Master in Pharmaceutical Care

Academic year: 2019 - 2020

**Optimization of a powder-based solid dosage form
of TNF- α siRNA-loaded lipidoid-polymer hybrid
nanoparticles designed for pulmonary delivery**

Laure Harinck

A Master dissertation for the study programme Master in Pharmaceutical Care

Academic year: 2019 - 2020

Master dissertation submitted to the Faculty of Pharmaceutical Sciences, performed in collaboration with the Laboratory Vaccine Design and Delivery, University of Copenhagen.

Promotor: Prof. dr. Koen Raemdonck

Second promotor: Prof. dr. Camilla Foged

Commissioners: Dr. Félix Sauvage and Dr. Evelien Wynendaele

The information, conclusions and points of view in this master dissertation are those of the author and do not necessarily represent the opinion of the promotor or his/her research group.

COPYRIGHT

"The author and the promoters give the authorization to consult and to copy parts of this thesis for personal use only. Any other use is limited by the laws of copyright, especially concerning the obligation to refer to the source whenever results from this thesis are cited."

Date

Promoter

Prof. dr. Koen Raemdonck

Prof. dr. Camilla Foged

Author

Laure Harinck

PREAMBLE

The experimental work presented in this thesis was performed at Department of Pharmacy, University of Copenhagen, Denmark, in the period from February 5 to May 29 with a break in the period from March 12 to April 26 due to the general COVID-19 lockdown in Denmark. The originally planned experiments included preparation and characterization of LPNs, spray drying, characterization of the spray-dried powders after reconstitution, solid state characterization, and determination of the flyability using PreciseInhale™. Due to the general COVID-19 lockdown in Denmark, it was not possible to be introduced to a part of the solid state characterization and determination of the flyability using PreciseInhale™. Hence, these experiments were performed by my colleagues You Xu (solid state characterization) and Aneesh Thakur (flyability). The data they obtained have been included in my thesis. In addition, I have not been able to repeat experiments, which means that the data presented in the thesis represent the results of only one experiment. This thesis has been finalized based on the acquired experimental data with additional description and discussion on the further steps that would have been taken if there was full lab time.

This preamble was formulated in consultation between supervisor and student and was approved by both.

ABSTRACT

Chronic obstructive pulmonary disease (COPD), which is characterized by chronic inflammation of the peripheral airways, is a major cause of death worldwide. The current therapies mainly provide symptom relief and do not alter the natural course of the disease. Therefore, there is an urgent need for novel treatment strategies. Tumor necrosis factor α (TNF- α) is a proinflammatory cytokine that amplifies inflammation and plays a central role in the pathophysiology of COPD. A potential therapeutic approach is silencing the gene expression of TNF- α by small interfering RNA (siRNA). Lipidoid-polymer hybrid nanoparticles (LPNs) are used as a safe and efficient delivery system to ensure intracellular delivery of siRNA to the target cells. Moreover, local delivery of the TNF- α siRNA-loaded LPNs by pulmonary administration is a rational approach to inhibit the TNF- α gene expression, since TNF- α is associated with inflammation of the lungs. In addition, it can provide a dose reduction of siRNA and thereby decrease the risk of systemic side effects. Hence, pulmonary delivery of inhaled medicines has become an attractive strategy for local treatment of COPD. The aims of this project were (i) to develop a powder-based solid dosage form of TNF- α siRNA-loaded LPNs for pulmonary delivery by optimizing the ratio of stabilizing excipients, *i.e.* trehalose and dextran, used during spray drying, and (ii) to characterize the aerosol performance of the dry powder formulations using the PreciseInhale™ (PI) system. The effect of different weight ratios of trehalose/dextran, used as stabilizing excipients during spray drying of the siRNA-loaded LPNs, was tested. Nanoparticle size, mass median aerodynamic diameter (MMAD), residual moisture content, surface morphology, and powder flyability were determined. The size ratio, comparing nanoparticle size after spray drying relative to before spray drying, showed a slight increase in particle size after spray drying. Hence, further experiments are needed to confirm the preservation of the structural integrity of the LPNs, and to investigate if the LPNs can be considered as sufficiently stable for safe and efficient delivery of siRNA to the target cells. The MMAD of the dry powder particles ranged from 3 to 4.5 μm , which implicates that the powder particles display an aerodynamic diameter suitable for deposition in the lower respiratory tract after inhalation. In addition, the results of the powder flyability tested in PI, showed that the aerosol performance was improved as the concentration of dextran, used as stabilizing excipient, was increased. This suggests the importance of dextran in the stabilization and the aerosol performance of the powder-based LPN formulations. However, additional characterization of the powder particles is needed to identify the optimal ratio of the carbohydrate excipients, trehalose and dextran, with the best aerodynamic properties and aerosol performance in PI. Nevertheless, this project was a promising start for future research to develop novel inhalable siRNA-based therapeutics for the treatment and management of COPD.

SAMENVATTING

Chronisch obstructieve longziekte (COPD) wordt gekenmerkt door chronische inflammatie van de perifere luchtwegen en leidt tot kortademigheid. Op dit moment is het de derde grootste doodsoorzaak ter wereld. De huidige behandelingen zijn vooral gebaseerd op het verlichten van de symptomen en hebben geen invloed op de progressie van de ziekte. Bijgevolg is er nood aan het ontwikkelen van nieuwe strategieën voor de behandeling van COPD. Tumor necrosis factor α (TNF- α) is een pro-inflammatoir cytokine dat een centrale rol speelt in de pathofysiologie van COPD. Een mogelijke therapeutische benadering bestaat uit de onderdrukking van de overexpressie van TNF- α via inhibitie van de post-translationale transcriptie door small interfering RNA (siRNA). Lipidoid-polymeer hybride nanopartikels (LPNs) worden gebruikt als een veilig en efficiënt transport systeem om siRNA intracellulair af te leveren in de target cellen. Bovendien kan lokale applicatie van de LPNs in de longen via inhalatie, zorgen voor een reductie in de therapeutische dosis siRNA. Bijgevolg leidt dit tot een verlaging van het risico op systemische neveneffecten. Vandaar dat pulmonaire administratie van geneesmiddelen wordt beschouwd als een aantrekkelijke strategie voor de lokale behandeling van COPD. De eerste doelstelling van het project was de productie van een op poeder gebaseerde doseringsvorm van LPNs, beladen met siRNA dat gericht is tegen TNF- α . Dit werd uitgevoerd door het optimaliseren van de ratio stabiliserende hulpstoffen, namelijk trehalose en dextran, die gebruikt werd tijdens het sproeidrogen van de formulaties. Vervolgens werden de aerosolisatie eigenschappen van de poeder formulaties gekarakteriseerd met behulp van het PreciseInhale™ (PI)-systeem. Het effect van de verschillende ratio's trehalose/dextran, gebruikt als stabiliserende hulpstoffen tijdens het sproeidrogen, werd getest. Dit werd gerealiseerd door de grootte van de nanopartikels, de massa mediane aerodynamische diameter (MMAD), het residuele watergehalte, de oppervlakte morfologie en de vliegbaarheid van de verkregen poeders te bepalen. De grootte verhouding van de LPNs (*i.e.* de grootte van de LPNs na het sproeidrogen ten opzichte van de grootte voor het sproeidrogen) toont een lichte verhoging van de partikelgrootte na het sproeidrogen. Bijgevolg is verder onderzoek nodig om behoud van de structurele integriteit van de LPNs te bevestigen. De MMAD van de poederpartikels bedraagt een waarde tussen 3 en 4.5 μm , wat aangeeft dat de verkregen poeders geschikt zijn voor afzetting in de onderste luchtwegen. Daarnaast tonen de resultaten van de testen in het PI-systeem aan dat aerosolisatie eigenschappen van het poeder verbeteren naarmate de concentratie dextran, gebruikt als stabiliserende hulpstof tijdens het sproeidrogen, verhoogt. Dit suggereert het belang van dextran in de stabilisatie en aerosolisatie van de LPNs in poedervorm. Verdere karakterisatie van de poederpartikels is echter nodig om de optimale ratio van stabiliserende hulpstoffen te definiëren, zodat een poeder bekomen wordt met de beste aerodynamische en aerosolisatie eigenschappen. Desondanks was dit een veelbelovend project voor toekomstig onderzoek naar de ontwikkeling van nieuwe inhalatie therapieën, gebaseerd op siRNA, voor de behandeling van COPD.

ACKNOWLEDGMENT

I would like to thank my supervisor Prof. Camilla Foged, for the warm welcome in the Vaccine Design and Delivery group in Copenhagen. I appreciate all the work she has done to guide me in the right direction and to give feedback whenever I needed it. Moreover, I am really grateful for all the opportunities she has given me to work on this project and to keep believing that I was going to be able to finish the project when the university closed due to the general COVID-19 lockdown.

Further, I would like to thank my co-supervisor Aneesh Thakur for all the feedback on my thesis and for all the time he has spent on generating data that I needed to complete my thesis when I was not allowed to go to the lab. Also, a special thanks to You Xu, who helped me during my experiments before the lockdown and performed the solid state characterization during the COVID-19 lockdown. She was always available to help me out with my questions.

A big thanks to Abhijeet Lokras to be available any time. He helped me a lot with interpretation of my data whenever it was needed. Also, even when I had to work alone in the lab due to the COVID-19 regulations, I could always call him to help me out with troubles finding the right material or operating the equipment.

I would like to thank Yibang Zhang and my fellow master students, Anas Aljabbari, Abishek Wadhwa and Siqi Feng for sharing their knowledge and for helping me in the lab. My stay in Copenhagen was a great experience thanks to all the positive vibes and optimism in the group. I will never forget all the nice moments we spent together as well as the running club during the lockdown, which I really enjoyed. I have learned more than I ever could have imagined not only about research but also about life and different cultures.

Finally, I am really grateful for all the support from friends and family back home. I want to thank my parents in particular, to encourage me in my decision to stay in Copenhagen during the lockdown due to COVID-19. This decision gave me the opportunity to finish as much as possible of my thesis and to enjoy the unique experience of Erasmus.

TABLE OF CONTENTS

PREAMBLE.....	
ABSTRACT	
SAMENVATTING	
ACKNOWLEDGMENT.....	
LIST OF ABBREVIATIONS	
1. INTRODUCTION.....	1
1.1. CHRONIC OBSTRUCTIVE PULMONARY DISEASE	1
1.2. siRNA AND THE RNA INTERFERENCE PATHWAY	2
1.3. DELIVERY OF siRNA.....	4
1.4. PULMONARY DELIVERY	7
1.5. SPRAY DRYING.....	8
1.6. AERODYNAMIC POWDER PROPERTIES.....	13
1.7. PRECISEINHALE™	15
2. OBJECTIVES.....	17
3. MATERIALS AND METHODS	19
3.1. MATERIALS.....	19
3.2. NANOPARTICLE PREPARATION AND PHYSICOCHEMICAL CHARACTERIZATION	19
3.3. SPRAY DRYING OF LPNs INTO NANOCOMPOSITE MICROPARTICLES	21
3.4. POWDER YIELD.....	21
3.5. REDISPERSIBILITY	21
3.6. SOLID STATE CHARACTERIZATION	22
3.7. AEROSOL GENERATION IN PRECISEINHALE™	23
3.8. PARTICLE SIZE DISTRIBUTION.....	23
3.9. STATISTICS	24
4. RESULTS	25
4.1. PREPARATION AND CHARACTERIZATION OF TNF- α siRNA-LOADED LPNs.....	25
4.2. SPRAY DRYING INFLUENCES THE PHYSICOCHEMICAL PROPERTIES OF THE TNF- α siRNA-LOADED LPNs	26
4.3. POWDER YIELD AND AERODYNAMIC PROPERTIES OF THE SPRAY-DRIED LPNs	28
4.4. SURFACE MORPHOLOGY OF THE SPRAY-DRIED LPNs.....	29
4.5. FLYABILITY OF NANOCOMPOSITE MICROPARTICLES	31

5.	DISCUSSION	33
6.	CONCLUSION AND FUTURE PERSPECTIVES	39
7.	REFERENCES.....	41

LIST OF ABBREVIATIONS

AGO2: Argonaute 2

APS: Aerodynamic particle sizer

C_{max} : Casella maximum concentration

COPD: Chronic obstructive pulmonary disease

DEPC: Diethyl pyrocarbonate

DESE: Double emulsion solvent evaporation

DOTAP: 1,2-dioleoyl-3- (trimethylammonium) propane

DPI: Dry powder inhaler

dsRNA: Double stranded ribonucleic acid

EDTA: Ethylenediaminetetraacetic acid

HD: Heparin-detergent

L_5 : Lipidoid 5

LPN: Lipidoid-polymer hybrid nanoparticle

MMAD: Mass median aerodynamic diameter

OG: Octyl β -D-glucopyranoside

PDI: Polydispersity index

PI: PreciseInhale™

PLGA: Poly(DL-lactic-co-glycolic acid)

pMDI: Pressurized metered dose inhaler

PSD: Particle size distribution

PVA: Polyvinyl alcohol

RISC: RNA-induced silencing complex

RNAi: Ribonucleic acid interference

SEM: Scanning electron microscope

siRNA: Small interfering ribonucleic acid

TE: Tris-ethylenediaminetetraacetic acid

T_g : Glass transition temperature

TGA: Thermogravimetric analysis

TNF- α : Tumor necrosis factor α

XRPD: X-ray powder diffraction

1. INTRODUCTION

In this chapter, the disease COPD will be discussed, including the pathophysiology, epidemiology, current treatments and novel therapeutic targets. Subsequently, the mechanism of RNAi using siRNA will be covered. Moreover, challenges in the delivery of siRNA and how they can be overcome by the use of multiple delivery systems will be presented. The use of LPNs as carrier for siRNA will be discussed more detailed. Furthermore, an explanation of the advantages, challenges, and requirements of pulmonary drug delivery for the local treatment of COPD will be provided. In addition, this chapter includes a discussion about the spray drying technique and the use of sugars as stabilizing excipients during spray drying. Furthermore, different devices available for administration of aerosolized drugs will be reviewed. Additionally, an overview of the possible experiments to investigate the aerodynamic powder properties, including NGI and PI, will be given.

1.1. CHRONIC OBSTRUCTIVE PULMONARY DISEASE

Chronic obstructive pulmonary disease (COPD) is a complicated disease of the lower respiratory tract. It is a common, treatable and preventable disease that is characterized by chronic inflammation of the peripheral airways and lung parenchyma (1, 2). Irreversible airflow limitation is a functional consequence of these airway and/or alveolar abnormalities, and it leads to shortness of breath (1-3). COPD is a major cause of comorbidity and mortality. The disease claimed 3.0 million lives in 2016, and it is currently the third-leading cause of death worldwide, according to the WHO (4). The condition is frequently underdiagnosed and undertreated, because many patients accept their limited exercise tolerance and breathlessness as symptoms of aging. Hence, the morbidity associated with COPD is underestimated, and an increase in the number of COPD patients is expected in the coming decades due to aging of the world's population and continued exposure to COPD risk factors (3, 5).

The most important risk factor for COPD is cigarette smoking (6). Smoking cessation can reduce the airflow limitation, but it is not fully reversible. Another main risk factor is associated with indoor air pollution caused by heating and cooking with biomass fuel, such as wood and coal (3). Especially women in developing countries are exposed to indoor air pollution, and the population at risk worldwide is large because almost three billion people use biomass and coal as energy source for heating and cooking. Other risk factors for the development of COPD are genetic factors (*e.g.*, different gene polymorphisms, including alpha-1-antichymotrypsin and TNF- α), age, sex, lung growth and development, and socioeconomic status (3, 6).

Current therapies for management of COPD are mainly based on the use of bronchodilators (β_2 -agonists and muscarinic receptor antagonists) associated with an anti-inflammatory agent (*i.e.* inhalation corticosteroids) (1, 7). However, these medications are focused on symptom relief and they do not treat the natural course of the disease. Hence, there is an unmet need for alternative therapeutic approaches that inhibit the chronic inflammation and prevent the progression of the disease or reverse the disease process. Advances in the understanding of the molecular mechanisms and cellular components involved in the pathogenesis of COPD have allowed for the identification of novel therapeutic targets (1, 7). The expression levels of many inflammatory mediators (*e.g.* cytokines, chemokines and growth factors) are increased in COPD. Tumor necrosis factor α (TNF- α) is a proinflammatory cytokine that amplifies inflammation (8). It is produced by alveolar macrophages, neutrophils, T cells, mast cells and epithelial cells. TNF- α is believed to play a central role in the pathophysiology of COPD, since it is correlated with cigarette smoke exposure, and it is capable of initiating inflammatory cascades during exacerbations of COPD. The concentration of TNF- α in sputum and serum increases in patients with COPD (2, 8).

Current therapeutic approaches based on inhibition of TNF- α includes anti-TNF biopharmaceuticals (*e.g.*, infliximab and etanercept). They are effective in the treatment of inflammatory diseases, *e.g.*, rheumatoid arthritis and inflammatory bowel disease, but the results of the first studies testing the TNF- α inhibitors in patients with COPD have not been very promising (9). Another disadvantage of this treatment is that the anti-TNF biopharmaceuticals may induce antibodies, which can result in undesired immunogenicity and eventually in response failure (10). Another approach is the use of ribonucleic acid interference (RNAi) therapy to inhibit TNF- α overexpression with small interfering RNA (siRNA) (9, 10).

1.2. siRNA AND THE RNA INTERFERENCE PATHWAY

The mechanism of RNAi was discovered in *Caenorhabditis elegans* in 1998 (11). The Nobel prize winners Andrew Fire and Craig Mello found that long double-stranded RNA (dsRNA) is able to silence gene expression in the nematode worm *C. elegans* (11, 12). The demonstration of RNAi in mammalian cells induced by short synthetic siRNA followed three years later (13, 14). In 2018, the first therapeutic drug based on siRNA was approved by the Food and Drug Administration. ONPATRO® (Patisiran), developed by Alnylam Pharmaceuticals, is an siRNA treatment for neuropathy in hereditary transthyretin amyloidosis in adults (15). This new class of therapeutics is based on silencing of specific disease-causing genes. Hence, 'undruggable' diseases can be treated by downregulating the expression of a target gene (*e.g.*, TNF- α) in a post-transcriptional way (16).

In the endogenous RNAi pathway of mammalian cells, long dsRNA is cleaved into siRNA by Dicer, which is an endonuclease of the RNase III family (17). siRNA are shorter fragments of 21-23 nucleotides in length. Once cleaved, the siRNA is loaded into the RNA-induced silencing complex (RISC) in the cytosol of the cell (16, 18). RISC contains multiple proteins, among others Argonaute 2 (AGO2). AGO2 cleaves the sense (passenger) strand from the duplex siRNA, which is subsequently degraded by nucleases in the activated RISC complex (16, 18). The remaining antisense (guide) strand in the RISC complex directs the complex to find the complementary base sequence of the target mRNA in the cell cytosol (16, 18). Upon binding of the antisense strand to the mRNA, AGO2 induces cleavage of the mRNA and causes post-transcriptional silencing of the target gene expression (16). After the cleavage, mRNA is released, and the antisense strand in RISC can be recycled for multiple cycles of mRNA cleavage (17). Hence, the RNAi pathway is very efficient, even at low doses of siRNA, and it has a large potential for highly specific knock down of its target (Figure 1.1.) (17, 18). Exogenous (synthetic) siRNA can be loaded directly onto the AGO2-RISC complex and thus bypass the previous steps in the RNAi pathway (13). Pulmonary diseases, *e.g.*, COPD, constitute potential therapeutic siRNA targets (*e.g.*, TNF- α). However, the delivery of exogenous siRNA into the cytosol of the cell faces a number of challenges (16).

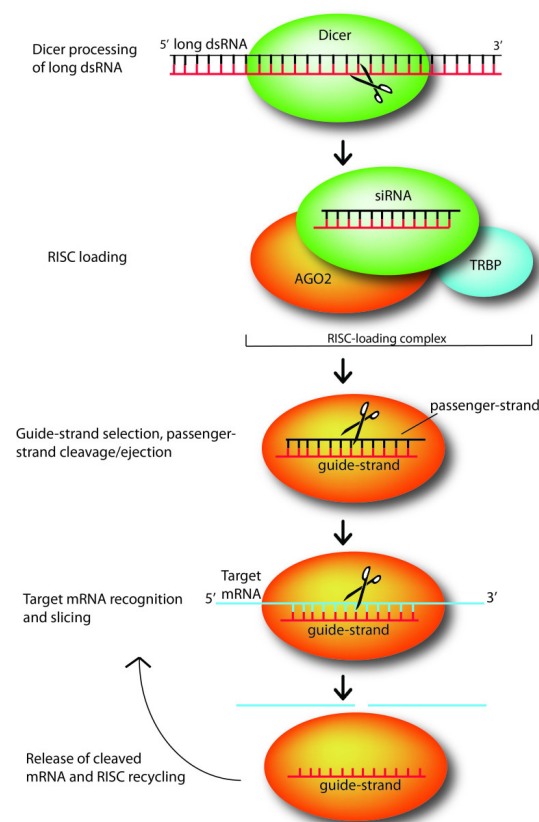


Figure 1.1: Mechanism of the RNAi pathway in the cytosol of mammalian cells (17).

1.3. DELIVERY OF siRNA

In theory, RNAi therapeutics can be designed to knock down the expression of any gene of interest in the body. Hence, they provide a broad spectrum of potential therapeutics for human diseases caused by overexpression of a gene, *e.g.*, autoimmune diseases, cancer, genetic disorders and viral diseases (17, 19). However, safe and efficient delivery of siRNA is one of the major challenges (17, 18). Unmodified siRNA (*i.e.* siRNA without any chemical modifications) is highly susceptible to degradation by endogenous nucleases present in biological fluids and tissues (18). Chemical modifications (*e.g.*, 2'-O-methyl modification in the ribose structure) can protect the siRNA from degradation by nucleases and increase the half-life. Another challenge is the intracellular delivery of siRNA to the RNAi pathway in the cytosol. An siRNA molecule has a large molecular weight (approx. 13-15 kDa) and is highly anionic owing to the negatively charged phosphate backbone. Due to these physicochemical characteristics, diffusion of siRNA across the cell membrane to the cytosol is not possible (17, 18). If the siRNA is taken up via endocytosis, there is an additional challenge of endosomal escape that needs to be overcome (17). Furthermore, unmodified siRNA is removed efficiently from the systemic circulation by the kidneys. It is subjected to rapid renal excretion because the pore size for glomerular filtration is approximately 8 nm (18). In addition, other hurdles, *e.g.*, activation of the immune system and off-target silencing (*i.e.* suppression of other genes than the target gene), needs to be taken into account (17, 18). To surmount these challenges, efficient delivery systems are necessary.

Throughout the years, multiple delivery systems have been developed. Viral vectors have been proven to be very efficient as delivery system. Nevertheless, there are safety concerns because they can cause host immunogenic and inflammatory responses, uncontrolled viral replication, tumorigenicity, and toxicity (16, 17). Due to these concerns, a lot of research has been done to develop effective non-viral delivery systems for siRNA. Some of the most important features of an adequate siRNA delivery system includes (i) protection of siRNA from enzymatic degradation, (ii) facilitation of cellular uptake, (iii) enhancing endosomal escape of siRNA into the cytosol, and (iv) avoiding off-target effects and toxicity (16).

A distinction can be made based on the way of administration of siRNA. Depending on the accessibility of the target tissue, local or systemic delivery may be preferred. Local siRNA delivery (*i.e.* direct delivery onto the target tissue) offers several advantages (20). For example, it can ensure a reduction of the dose of siRNA necessary for effective gene silencing, and thereby a reduction of the systemic adverse effects. Tissues suitable for local therapy include mucus membranes, eyes and skin (20). Possible siRNA delivery approaches for local administration comprise unmodified siRNA and siRNA conjugates. However, many tissues are not accessible

through local delivery and therefore systemic administration is necessary (20). Systemic delivery faces multiple hurdles previously described in this section (*e.g.*, renal clearance, aggregation with blood components, enzymatic degradation by endogenous nucleases, and uptake by phagocytes) (20, 21). Therefore, a large variety of delivery systems are available to protect siRNA from degradation and to improve cellular uptake in the target tissue. The most commonly applied delivery systems up till now include lipoplexes and liposomes (13), SNALPs (19), polymeric nanoparticles (17), and conjugates enabling targeting cells of interest (17).

For this study, a delivery system based on lipidoid-polymer hybrid nanoparticles (LPNs) was used. Poly(DL-lactic-co-glycolic acid) (PLGA) is a polymer frequently used for the preparation of polymeric nanoparticles (22). It is a copolymer containing the two different monomers glycolic acid and lactic acid. PLGA undergoes hydrolysis in the body into these two monomers, which are metabolized via the Krebs cycle. Therefore, PLGA is one of the most effective biodegradable polymers and displays low toxicity and high biocompatibility with cells and tissues (22). Furthermore, other important advantages of PLGA nanoparticles include protection of siRNA from nuclease degradation (23), and sustained and controlled release of encapsulated siRNA (24). However, as a consequence of the anionic nature of PLGA, encapsulation of negatively charged siRNA is challenging. Hence, modification of PLGA nanoparticles with cationic lipids, *e.g.*, 1,2-dioleoyl-3-(trimethylammonium) propane (DOTAP), leads to improved encapsulation efficiency because anionic siRNA is loaded into the nanoparticles through attractive electrostatic interactions with the cationic lipids (23). In addition, the cationic lipid component provides an enhanced transfection efficiency due to improved cellular uptake and membrane permeation, which is caused by interaction of the positive charges of the lipid headgroups with the negatively charged cell surface (25, 26).

Depending on the method used for preparation, the structure of LPNs has been suggested to comprise a polymeric core and an outer lipid shell layer (27). Due to combination of the characteristics of both polymeric nanoparticles and liposomes, LPNs constitute an siRNA delivery system with superior *in vivo* cellular delivery efficiency. The polymeric core ensures structural integrity and controlled release properties, while the lipid shell layer provides biocompatibility and bioavailability (27). Despite the advantages of the integration of cationic lipids into the polymeric nanoparticles, they can cause an excessive positive charge. This can lead to several problems including non-specific protein binding, and toxicity (28). In detail, frequently used cationic lipids *e.g.*, DOTAP, display a single quaternary ammonium group, which is proven to be more toxic than tertiary amines (29). This quaternary ammonium group causes a high positive charge. As a consequence, non-specific serum proteins can bind to the positively charged nanoparticles, which provides neutralization of the particles, and an increase

in particle size (29). This may result in reduced transfection efficiency caused by neutralization, and cellular toxicity due to the large particle size. Furthermore, cells can recognize the high density of positive charges at the surface of the nanoparticles as a signal to trigger proinflammatory reactions and to activate intracellular signaling pathways, leading to toxicity (26).

Hence, a novel class of lipid-like materials termed *lipidooids* has been designed (28). These compounds consist of an alkylated tetraamine backbone (Figure 1.2). Different analogues are obtained, depending on the degree of alkylation, *e.g.*, tetra-alkylated lipidoid (L_4) consisting of an alkylated backbone with four alkyl chains, penta-alkylated lipidoid (L_5), and hexa-alkylated lipidoid (L_6), which is fully alkylated (30). Compared to commonly used cationic lipids, *e.g.*, DOTAP, lipidoids contain multiple secondary and tertiary amines. Therefore they are more efficient in interacting with anionic siRNA molecules without significantly increasing the net charge of the LPNs (28). Consequently, the encapsulation efficiency of siRNA is enhanced and thus a lower effective dose of cationic lipid in lipidoid-LPNs is needed, compared to DOTAP-LPNs at an equimolar dose of siRNA (10). As a result, toxic side effects caused by the cationic lipids are reduced. Furthermore, integration of the lipidoids into the LPNs provide an enhanced intracellular delivery of siRNA, rendering them more transfection-competent in contrast to DOTAP (10). Hence, a more efficient gene silencing might be obtained, which allows for a dose reduction and leads to improvement of the safety and efficacy of the delivery system (10). The L_5 -modified LPNs exhibited the strongest *in vitro* gene silencing effects, and were more efficient compared to DOTAP-modified LPNs (28).

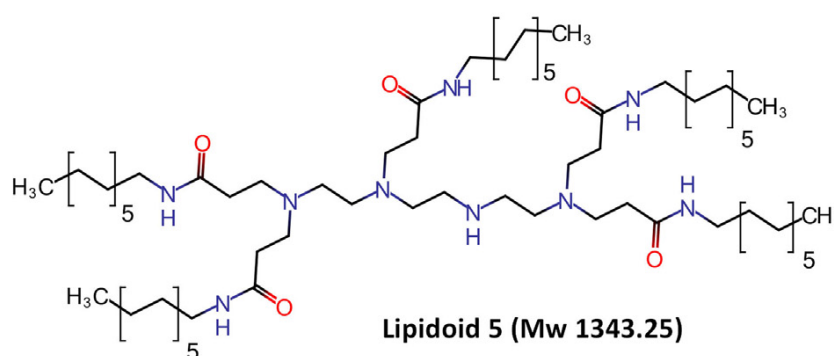


Figure 1.2: Structure of lipidoid 5 (L_5) (nitrogen=blue; oxygen=red; carbon=black, colored according to CPK coloring) (28).

A variety of different methods can be used for the preparation of LPNs. Among the most applied strategies, a distinction is made between one-step and two-step methods, respectively. For the one-step method, lipid and polymer solutions are mixed directly, and the components tend to form LPNs based on self-assembly. In contrast, for the two-step method, the polymeric nanoparticles and the lipid vesicles are prepared separately and subsequently mixed. General strategies adopting both one- and two-step methods comprise nanoprecipitation, high-pressure homogenization and emulsification-solvent evaporation (ESE), which can be subclassified into single and double ESE. The use of microfluidics is a novel approach, which can be classified as a one-step method (31).

In this project, lipidoid-PLGA hybrid nanoparticles, composed of L_5 and PLGA, were prepared by using the double emulsion solvent evaporation (DESE) method (32). DESE enables efficient encapsulation of polyanionic and water-soluble compounds (*e.g.*, siRNA). In the first step, a primary water-in-oil (w/o) emulsion is formed by mixing an aqueous phase containing polyanionic siRNA with an organic phase containing hydrophobic PLGA and cationic L_5 . The second step involves phase inversion and stabilization of a secondary emulsion. The primary w/o emulsion is emulsified into a second aqueous phase containing the surfactant polyvinyl alcohol (PVA), which provides stabilization. Subsequently, a size reduction with probe sonication is necessary, because phase inversion causes increased droplet size of the emulsion. At last, the organic solvent is evaporated by stirring, eventually resulting in an LPN dispersion (32, 33).

1.4. PULMONARY DELIVERY

Pulmonary drug delivery of therapeutic nanoparticles is a promising strategy to treat pulmonary or systemic diseases (34). This strategy can be used to achieve either local or systemic effects and offers several advantages. First, it constitutes a non-invasive method of administration, which provides the opportunity to avoid the adverse effects and inconvenience of parenteral administration, hence improving patient compliance (34). In addition, the lungs are characterized by (i) a large surface area, (ii) high vascularization, and (iii) a thin alveolar epithelium. These characteristics result in efficient and fast drug absorption, which is attractive for systemic delivery (35). In this study, the aim was to design TNF- α siRNA-loaded LPNs for the local treatment of COPD via pulmonary administration. The hypothesis is that due to the direct deposition of the LPNs to the target cells, a reduction in siRNA dose may be possible, thereby decreasing the risk of undesired systemic side effects (36).

The LPNs interact with alveolar macrophages, epithelial cells and lung surfactant in the lower airways after pulmonary administration. Mainly the macrophages are promising targets for silencing the expression of genes responsible for inflammation in COPD (*e.g.*, TNF- α) (37).

However, delivery of LPNs in the lower respiratory tract encounters a number of challenges because the lungs are equipped with several defense mechanisms to clear inhaled particles and protect the airways (38). The primary defense mechanism is mucociliary clearance (39). The respiratory tract is divided into two parts, *i.e.* the upper respiratory tract and the lower respiratory tract. Another possible division of the airways is based on the ability to exchange gas. The conducting zone consists of the upper respiratory tract together with a part of the lower respiratory tract, namely the tracheobronchial airways. On the other hand, the respiratory zone includes the respiratory bronchioles, alveolar ducts and alveoli (39). Mucociliary clearance removes inhaled particles from the conducting zone (36, 38). The airway surface comprises two components. The first one is the mucus layer, which consists of cross-linked mucin fibers, and it is responsible for the entrapment of the inhaled particles. The second component is the periciliary layer containing cilia, which beat in coordinated metachronal waves to provide continuous transport of the mucus. In 24 h, all deposited material in the tracheobronchial airways is transported towards the throat, where it is expectorated or swallowed (36, 38, 39).

Other defense mechanisms include cough, degradation of inhaled particles by proteolytic enzymes and alveolar macrophages, and anatomical barriers of the respiratory tract (38, 39). Due to the anatomically branched structure of the lungs, controlling the deposition of drug-containing particles can be challenging. Therefore, inhaled LPNs need to display appropriate morphological and aerodynamic characteristics (40). The particle size of the LPNs is one of the most important parameters, and it is usually referred to as the aerodynamic diameter. An aerodynamic diameter between 1 and 5 μm is required to reach the deep lungs (41). Larger particles (> 5 μm) are deposited in the upper airways, whereas particles with an aerodynamic diameter below 1 μm are mainly exhaled during breathing (40, 41). Therefore, it is necessary to have an appropriate technique to manufacture a solid dosage form of LPNs with aerodynamic and morphological properties customized for inhalation.

1.5. SPRAY DRYING

Several drying technologies are available for the preparation of solid dosage forms of nanoparticles. The most commonly used drying methods include spray drying, freeze drying, spray-freeze drying, and supercritical fluid drying (42). Spray drying is an attractive process for the manufacturing of solid dosage forms of

nanoparticles suitable for inhalation (43). This method has several advantages because it is a rapid, single step, cost-effective, simple, and reproducible process (42). Moreover, it allows particle engineering of the powder particles, which enables the production of spray-dried powders with a mean aerodynamic diameter appropriate for deep lung deposition (44). In addition, it is an attractive process in both laboratory and industrial settings, because it represents an easily scalable process, and a wide spectrum of compounds (including heat-sensitive materials) can be spray dried (43).

During the spray drying process, the liquid feed is transformed into a dry particulate form by atomization of the feed in a hot drying medium. The process can be divided into four main phases: (i) atomization of the liquid feed into droplets, (ii) contact of the droplets with a hot drying gas, (iii) dry particle formation, and (iv) collection of the dry product by separation from the drying gas (45, 46). The liquid feed is transported to the atomizer or nozzle using a peristaltic pump. The nozzle ensures breaking of the liquid feed into small droplets, offering the formation of large surface areas (47). Consequently, quick evaporation of the solvent occurs. In detail, efficient heat transfer from the drying gas to the droplets is possible due to the large net surface area. Therefore, the droplets reach lower temperatures compared to the inlet temperature of the drying gas. Hence, spray drying is useful for drying of heat-sensitive compounds due to the atomization step. After atomization, contact between the droplets and the hot drying gas occurs in the drying chamber. As a consequence, the moisture content of the droplets is evaporated, resulting in dry powder particles (43). In this study, nitrogen is used as drying gas. Furthermore, a co-current drying chamber is operated. This dryer is characterized by the placement of both the drying gas inlet and the nozzle in the upper part of the chamber (47). Therefore, the atomized liquid feed comes into contact with the highest temperature of the drying gas, while the dry particles are the least heated (43). This is recommended for drying of heat-sensitive compounds. It is a universal type of drying chamber and it is frequently used (47). Finally, the produced particles are separated from the gas stream using a cyclone. Centrifugal forces present in the cyclone ensure deposition of the particles towards the walls of the device. Reduction of powder accumulation on the wall of the cyclone is prevented by a special coating on the inside of the cyclone (47). Subsequently, the particles are collected into a collection vessel located at the bottom of the spray dryer (43).

Three process parameters display the main influence on the physicochemical and morphological powder properties of the resulting powders. In particular, (i) the inlet temperature, (ii) the nozzle gas flow rate, and (iii) the feed flow rate, can be optimized to achieve the desired characteristics of the dry powder particles (*i.e.* particle

size, powder yield, and residual moisture content) (Figure 1.3) (48). In this project, previously optimized process parameters were used for spray drying (49).

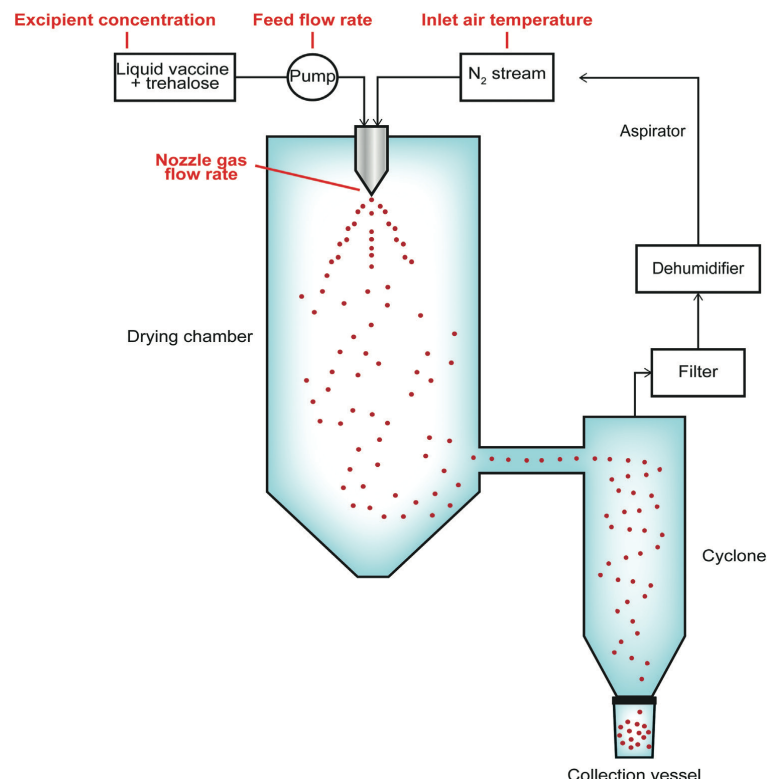


Figure 1.3: Illustration of the spray drying process. The three main process parameters and one formulation parameter (*i.e.* excipient concentration) are identified in red (48).

Drying of the nanoparticles causes improvement of stability during long-term storage (50). However, during the spray drying process, the LPNs are exposed to high temperatures and shearing forces, which can cause destabilization of the nanoparticles. Therefore, stabilizing excipients, *e.g.*, sugars, are required to preserve the physical stability (50). Furthermore, stabilizers ensure the possibility of rehydration (50, 51). If the nanoparticles are dehydrated without the presence of an excipient, aggregation, fusion, and leakage of the encapsulated drug in the LPNs may occur. Hence, protective excipients are applied to avoid this. In particular, membrane fusion is prevented due to the presence of carbohydrates as they conserve partially the original hydrated condition (52). Consequently, the size of the spray-dried nanocomposite microparticles [*i.e.* drug-encapsulated nanoparticles dispersed in a microparticle carrier *e.g.*, carbohydrates (51)] is maintained and remains suitable for deep lung delivery (50, 51). The biocompatible saccharides of the nanocomposite microparticles dissolve in the lung-lining fluid after pulmonary administration, and the embedded nanoparticles are released (Figure 1.4) (51, 53). Moreover, applying high inlet temperatures during spray drying can lead to shrinkage and collapse of the LPNs,

resulting in smaller particles. This collapse and decrease in size can be avoided by adding sugars (51). Additionally, sugar excipients can serve as a bulking agent to obtain a sufficient amount of powder suitable for inhalation (54).

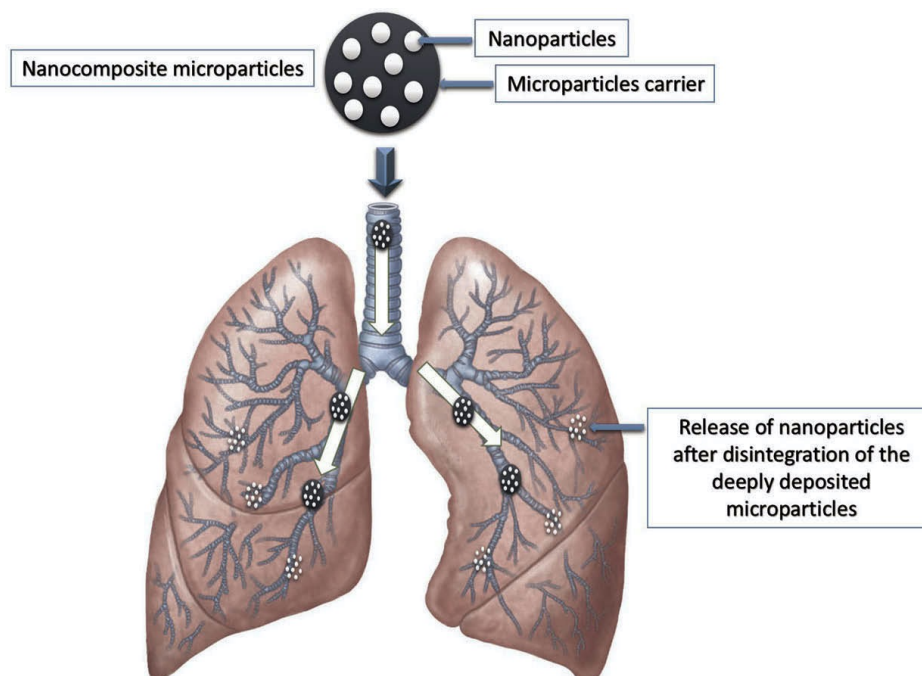


Figure 1.4: Illustration of the structure of nanocomposite microparticles and the mechanism of release of the nanoparticles after pulmonary administration (51).

Carbohydrates are suggested to stabilize nanoparticles during spray drying mainly via two different mechanisms (Figure 1.5). First, the water replacement theory is based on the ability of the stabilizing excipient to replace the hydrogen bonds of the water molecules to the nanoparticles (Figure 1.5A) (50). In detail, the LPNs are stable under hydrated conditions. However, during spray drying, the water evaporates, and the nanoparticles can lose their structural integrity by forming intramolecular hydrogen bonds (52, 55). The excipient serves as a substitute for water because the hydroxyl groups of the carbohydrates form hydrogen bonds with the polar headgroups of the lipids incorporated in the nanoparticles (50). As a result, the structure of the LPNs is preserved, eventually resulting in enhanced storage stability (56). Second, the vitrification theory uses the principle of changes in reaction kinetics (Figure 1.5B) (57). Sugars are able to form an amorphous, glassy matrix surrounding the nanoparticles. Hence, the nanoparticles are immobilized, and as a consequence, degradation is slowed down since molecular mobility is required for degradation and aggregation of nanoparticles (56, 57). Both theories cannot totally explain the stabilization of the nanoparticles and hence they should be considered simultaneously (52, 58).

molecular weight of the carbohydrate increases, the T_g increases as well (55). Trehalose is a non-reducing disaccharide consisting of two glucose units. With a T_g value of 117 °C, it is the disaccharide with the highest T_g (60). Even if the T_g decreases due to the presence of residual moisture, it will remain above the storage temperature and provide stability. Therefore, trehalose can be considered as a good stabilizing excipient (58). On the other hand, polysaccharides, *e.g.*, high-molecular weight dextrans, have even higher T_g values and easily form amorphous matrices (55). Nevertheless, they are considered as poor stabilizers (61). Due to their large size and rigidity, their ability to form hydrogen bonds with the nanoparticles is limited because of steric hindrance (Figure 1.6) (55). Oligosaccharides are able to combine both advantages of disaccharides and polysaccharides, *i.e.* a high molecular flexibility to maintain hydrogen bonds with the particles, and a high T_g to achieve a glassy matrix (61). As a consequence, a more compact coating of the particle can be achieved, resulting in a higher stability of the formulation (55). Furthermore, disaccharides (*e.g.*, trehalose) and polysaccharides can be combined to obtain an increase in T_g and improve the coating of the particles (62).

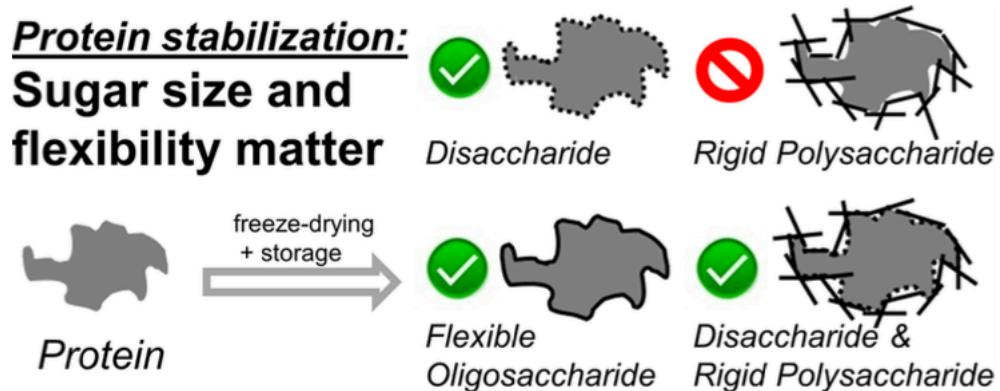


Figure 1.6: Illustration of the influence of size and molecular flexibility of different sugars (*e.g.*, disaccharides, oligosaccharides, and polysaccharides) on the compactness of the nanoparticle coating (55).

1.6. AERODYNAMIC POWDER PROPERTIES

In addition to the stability, also the flyability of the resulting powders should be considered and optimized. To deliver drugs by inhalation, aerosols need to be generated and administered to the lungs. Mainly three delivery devices *i.e.* nebulizers, pressurized metered dose inhalers (pMDI), and dry powder inhalers (DPI), are available to administer aerosolized drugs to the respiratory tract (63).

First, nebulizers are devices that generate an inhalable aerosol by converting liquids into small droplets using compressed gas or ultrasonic vibration (64). They provide continuous production of aerosols, hence these

devices are suitable for unconscious, elderly, and acutely ill patients (46, 65). However, nebulizers are associated with several disadvantages including (i) not portable, (ii) noisy, (iii) an outside energy source can be required, and (iv) longer treatment times compared to pMDI and DPI (65). Therefore, this type of device is usually reserved for treatment in hospital (46).

Second, pMDIs are designed to deliver a metered dose of an aerosol generated by using a propellant under pressure (64). The main advantage is that it is a compact and portable device, which allows patients to use it discretely and in acute situations (46). On the other hand, some important disadvantages are associated with the device. For example, it requires coordination of inhalation and actuation of the device. Some people, *e.g.*, elderly, are unable to perform good coordination, which results in reduced drug delivery (65). Furthermore, due to the rapid expansion of the propellant after actuation of the device, the aerosol spray has a high initial velocity, resulting in a higher deposition of the drug into the mouth and oropharynx (46). As a consequence, a decrease of drug deposition in the respiratory tract is feasible.

Last, DPIs are breath-actuated devices (65). When the patient inhales, dry powder aerosols are created via the airstream and deposited into the lungs. Hence, the coordination-related problems characteristic for pMDIs are avoided. However, a certain inspiratory effort is essential, and therefore these devices are unsuitable for patients with severe respiratory conditions (65).

It has been reported that DPIs are better, compared to pMDIs and nebulizers, with respect to aerosol performance and physicochemical stability of the dosage form (66). Furthermore, the aerosolization properties of the drug particles in DPIs depend on both the inhaler device and the powder formulation (67). As previously described in this introduction (section 1.4 Pulmonary delivery), the aerodynamic properties of the inhalable powders are of main importance to provide particle deposition into the deep lungs. Aerosolized particles with an aerodynamic diameter ranging from 1–5 μm are required (68). Therefore, spray drying is an attractive particle engineering technique, which allows for the production of inhalable powders with high flyability and desired aerodynamic properties (68, 69). Hence, investigation of the aerosolization performance and aerodynamic properties is necessary to ensure that the inhalable particles are suitable for pulmonary delivery (69, 70).

Cascade impactors are the most commonly used instruments to investigate aerosolization *in vitro* (71). Different cascade impactors for the aerodynamic assessment of fine particles are described in the European Pharmacopeia (section 2.9.18), including the Next Generation Impactor (NGI) (72). An inhaler device, used to

generate the aerosols, is connected to the NGI (70). Subsequently, the impactor fractionates the aerosols based on particles size, ranging from 0.1 – 12 μm in aerodynamic diameter, and provides the determination of an aerodynamic particle size distribution (PSD) (73). The PSD data might enable prediction of the lung deposition pattern of the inhaled particles in humans (71). Furthermore, the mass median aerodynamic diameter (MMAD) can be calculated from the obtained NGI data (69). However, for each test, approximately 10 mg of powder is needed (70), which can be a disadvantage when only a limited amount of test powder is available.

1.7. PRECISEINHALE™

The PreciseInhale™ (PI) equipment is a newer instrument that can be used to generate aerosols and determine the flyability of inhalable powders (Figure 1.7). This system allows well-controlled powder aerosol exposures using a DustGun aerosol technology (74). Small amounts of powder are aerosolized by using compressed air causing respirable aerosols available for exposure in a broad range of exposure models. The choice of model is depending on the desired inhalation experiments, *e.g.*, exposure and dissolution testing *in vitro*, lungs *ex vivo*, and animals *in vivo* (75). An advantage, compared to the generally used instruments like the NGI, is that only a small amount of powder is needed to determine the aerodynamic properties of the powder (76).

The small amount of powder is loaded into the powder chamber of the PI platform (Figure 1.7). Subsequently, a jet of high-pressure air is shot through the powder chamber (Figure 1.7, 1), de-agglomerating and swirling up the powder, and ejecting it through the exit nozzle into a cylindrical holding chamber (Figure 1.7, 2). At the base of the holding chamber, there is an exposure line. When the pressure between the powder and the holding chamber is equalized, the generated aerosols swirl downwards in the holding chamber (Figure 1.7, 3). An adjustable airflow, controlled via a vacuum pump (Figure 1.7, 5), pulls the aerosol cloud out of the holding chamber, and subsequently, the aerosolized powder can be transferred to the cells/animals for experiments, or it can be collected for analysis (77, 78). A Marple Cascade Impactor is coupled to the PI platform to determine the particle size distribution of the generated aerosol (79). The particles are pumped through the Marple Cascade Impactor at an airflow rate of 2 l/min (Figure 1.7, 4). Based on the size of the particles, they are captured by impaction on the different stages of the impactor. Consequently, the MMAD can be calculated from the mass of particles deposited on each stage of the impactor (79, 80).

While the generated aerosol passes through the exposure line, a light-scattering device (Casella) is used to measure the aerosol concentration (81). In addition, the ventilation pattern of the exposed animal can be

monitored using a control program. Due to these two factors (*i.e.* measurement of the aerosol concentration and determination of the ventilation pattern), precision dosing is allowed (76). Since the experiments using PI are performed in one exposure subject at the time, precision dosing provides high reproducibility and accurate dosing of the dry powder into the lungs (74). This suggests that the PI method can be used to investigate the effect of drugs in different exposure models (78). Furthermore, only small amounts of powder are needed, hence it is a suitable technology when limited amount of test powder is available (76).

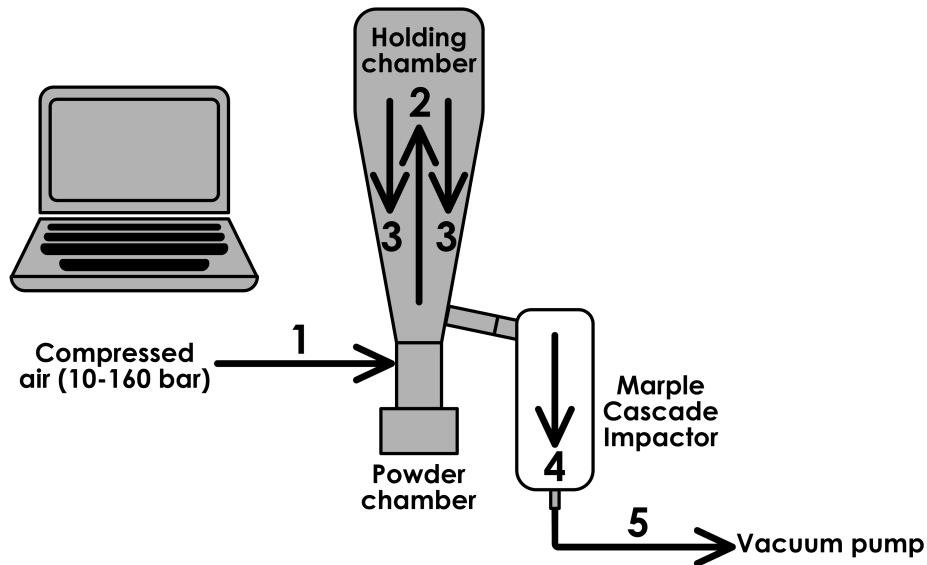


Figure 1.7: Preciselnhale™ (PI) system connected to a Marple Cascade Impactor. A high-pressure air jet is shot through the powder chamber (1), causing de-agglomeration and swirling up of the powder into the holding chamber (2). Subsequently, the generated aerosols swirl downwards (3), and the particles are pumped through the Marple Cascade Impactor (4). A vacuum pump is used to generate an adjustable airflow, which pulls the aerosols out of the holding chamber (5) (75).

Mainly three settings in the PI system influence powder flyability, *i.e.* (i) the generation pressure, (ii) the reset pressure, and (iii) the plunger displacement (49). The generation pressure is defined as the initial pressure shot through the powder chamber, while the reset pressure is known as the pressure level established after exposure. In addition, the plunger displacement allows adjustment of the volume of the high-pressure chamber. By controlling these three settings, the volume and dose of the generated aerosol ejected into the holding chamber can be regulated (49).

2. OBJECTIVES

COPD is a pulmonary disease characterized by chronic inflammation of the peripheral airways, which causes irreversible airflow limitation and shortness of breath (1, 2). It is currently the third-leading cause of death worldwide (4). Moreover, according to the WHO, there were 3.0 million deaths in 2016 due to the disease. The therapies available for management of COPD (*e.g.*, bronchodilators and anti-inflammatory agents) mainly provide symptom relief (1). However, there is an unmet need for novel treatment strategies, which can be used to treat the natural course of the disease, *e.g.*, inhibition of chronic inflammation and prevention or reversal of the disease progression (7).

TNF- α is a proinflammatory cytokine capable of initiating inflammatory cascades during exacerbations of COPD (8). A possible therapeutic approach is the inhibition of TNF- α overexpression using siRNA in the RNAi pathway (9, 10). Specifically, siRNA is able to silence specific disease-causing genes by binding to the complementary nucleotide sequence of the target mRNA, and subsequently inducing cleavage of the mRNA. Hence, a post-transcriptional downregulation of the expression of the target gene is provided (16). However, a major challenge is the intracellular delivery of exogenous siRNA to the RNAi pathway in the cytosol of the target cells (18). Due to the large molecular weight and anionic characteristics of siRNA, diffusion across the cell membrane is not possible. Furthermore, siRNA is sensitive to degradation by endogenous nucleases. To overcome these hurdles, safe and efficient delivery systems *e.g.*, lipidoid-polymer hybrid nanoparticles (LPNs), are necessary.

Pulmonary administration of LPNs is an attractive strategy for local treatment of COPD (34). The hypothesis is that due to direct deposition of TNF- α siRNA-loaded LPNs to the target cells, a reduction in siRNA dose may be possible, thereby decreasing the risk of undesired systemic side effects (36). However, the lungs are equipped with several defense mechanisms to clear inhaled particles, *e.g.*, the anatomical branched structure of the respiratory tract (38). Hence, these challenges need to be surmounted to deliver the LPNs into the deep lungs. Therefore, the aerodynamic characteristics of the inhaled LPNs are of main importance. An aerodynamic diameter between 1 and 5 μm is required to obtain suitable delivery of the nanoparticles into the lower respiratory tract (41). Furthermore, good aerosolization properties of the LPNs are essential to obtain appropriate particle deposition into the lungs after administration with an inhalation device.

The purpose of this project was to optimize the aerosolization properties of a powder-based solid dosage form of TNF- α siRNA-loaded LPNs suitable for pulmonary delivery by using the spray drying technique. The hypothesis is that by optimizing the ratio of the carbohydrate excipients, *i.e.* the disaccharide trehalose and the polysaccharide dextran, used to spray-dry the LPNs, an increase in T_g and a better coating of the nanoparticles can be achieved, resulting in a higher stabilization of the formulation. Hence, nanocomposite microparticles will be generated with aerodynamic and aerosol properties suitable for pulmonary administration. The specific aims of this project were (i) to manufacture a solid dosage form of nanocomposite microparticles with appropriate aerodynamic characteristics for pulmonary delivery by using the spray drying technology, and (ii) to characterize the aerosol performance of the obtained dry powder formulations using the PI system.

In this study, formulations of TNF- α siRNA-loaded LPNs were prepared by using the DESE method. The LPNs were spray-dried into nanocomposite microparticles (powder) using a binary mixture of carbohydrate excipients consisting of the disaccharide trehalose and the polysaccharide dextran at different weight ratios. The physicochemical properties of the obtained nanoparticles were measured twice, *i.e.* before and after spray drying. This was performed to investigate if the spray drying process influences the nanoparticle characteristics. To measure the physicochemical properties after spray drying, the nanocomposite microparticles were redispersed into a homogenous suspension of LPNs by adding a volume of water resulting in a final solid concentration identical to the solid concentration before spray drying. Dynamic light scattering was used to determine particle size and PDI, whereas zeta potential was measured using laser-Doppler microelectrophoresis. Furthermore, the siRNA encapsulation efficiency of the LPNs was measured by fluorescence spectroscopy using the RiboGreen[®] RNA reagent and a fluorescence plate reader.

To characterize the powder properties of the obtained solid dosage form after spray drying, solid state characterization was performed including (i) measurement of the aerodynamic particle size using an Aerodynamic Particle Sizer (APS) Spectrophotometer, (ii) investigation of the residual moisture content by thermogravimetric analysis (TGA), (iii) determination of the surface morphology by scanning electron microscopy (SEM), and (iv) investigation of powder crystallinity using X-ray powder diffraction (XRPD). The most optimal powder displaying the desired aerodynamic and aerosolization properties suitable for inhalation was selected after investigation of the flyability of the resulting powders using the PI system.

3. MATERIALS AND METHODS

3.1. MATERIALS

2'-O-methyl-modified dicer substrate asymmetric siRNA duplex directed against tumor necrosis factor α (TNF- α siRNA, 18 g/mol) was provided as a dried, purified and desalted duplex from GlaxoSmithKline (Stevenage, UK). L₅ was synthesized, purified and characterized as reported previously (28). PLGA (lactide:glycolide molar ratio 75:25, Mw: 20 kDa) was purchased from Wako Pure Chemical Industries (Osaka, Japan). Polyvinyl alcohol (PVA) was obtained from Sigma-Aldrich (St. Louis, MO, USA). Heparin-detergent (HD) solution contains heparin (1 mg/ml) (Biochrom GmbH, Berlin, Germany) and octyl β -D-glucopyranoside (100 μ M) (OG) (Sigma-Aldrich). Tris-EDTA buffer (10 mM Tris, 1 mM EDTA, pH 7.5) (TE buffer) and Quant-iT™ RiboGreen® reagent were provided by Molecular Probes, Invitrogen (Paisley, UK). RNase-free diethyl pyrocarbonate-water (DEPC) was used for all dilutions and solutions. Carbohydrate excipients used for spray drying included trehalose dihydrate (Sigma-Aldrich) and dextran (6 kDa, Alfa Aesar, Haverhill, MA, USA). Additional chemicals were of analytical grade and provided by Sigma-Aldrich.

3.2. NANOPARTICLE PREPARATION AND PHYSICOCHEMICAL CHARACTERIZATION

The TNF- α siRNA-loaded LPNs were prepared by using the double emulsion solvent evaporation method (DESE) as previously reported (Figure 3.1) (32). Briefly, the primary emulsion (w/o) is obtained by adding a mix of 8.3 μ l siRNA in 116.7 μ l TE buffer to 250 μ l of CH₂Cl₂ containing 2.25 mg L₅ and 12.75 mg PLGA. The L₅ content relative to the total solid content (L₅ + PLGA) was kept at 15% (w/w) and the L₅:siRNA ratio was constant at 15:1 (w/w). The primary emulsion was sonicated in an ice bath using a probe sonicator (Misonix, Qsonica, LLC., CT, USA) for efficient mixing and maximizing the hydrophobic and electrostatic interactions between the organic and aqueous components. The probe sonicator was set at 90 s with an amplitude of 50. To obtain a phase inversion of the primary emulsion and formation of the secondary w₁/o/w₂ emulsion, 1 ml of PVA solution was added. The mixture was vortexed for 1 min, and the resulting emulsion was probe-sonicated in an ice bath for 90 s with an amplitude of 30. Subsequently, the emulsion was transferred into an RNase-free glass beaker containing a magnet, and a volume of 5 ml PVA solution was added to the nanoparticle dispersion. The dispersion was stirred for 45 min to allow for evaporation of CH₂Cl₂. To remove unencapsulated siRNA and PVA, the LPN dispersion was purified by centrifugation using a gradient centrifugation method, *i.e.*, 6000 g for 5 min, 12000 g for 5 min, 21000 g for 5 min, 34000 g for 5 min, and 48000 g for 10 min at 4 °C. The LPNs were immediately resuspended in 500 μ l DEPC-water by using a vortex and bath-sonication. The formulations with a total volume of 2 ml were stored at 4 °C.

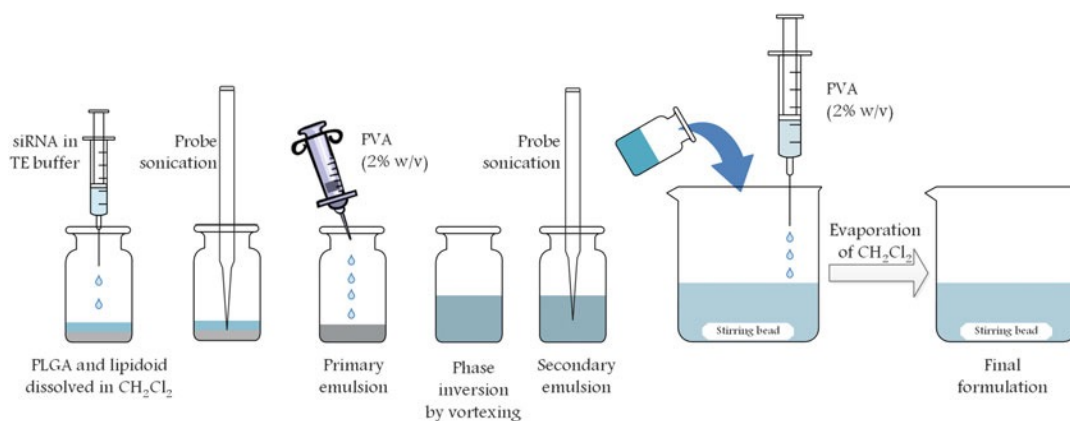


Figure 3.1: Illustration of the DESE used for preparation of LPNs (32).

The intensity-weighted mean hydrodynamic diameter (z -average) and the polydispersity index (PDI) were measured by dynamic light scattering using the photon correlation spectroscopy technique. For the size analysis, the samples were diluted 40 times with DEPC-water. All measurements were repeated three times per sample at 25 °C using a Zetasizer® Nano ZS (Malvern Instruments, Worcestershire, UK) equipped with a 633 nm laser and 173° detection optics. For analyzing and collecting data, the Malvern Zetasizer® software (version 7.11) was used. The particle size distribution was reflected in the PDI, which ranges from 0 for a monodisperse to 1 for a completely heterogeneous sample. The zeta potential of the LPN dispersion was measured using laser-Doppler micro-electrophoresis. The measurements were performed in triplicate and the Malvern Zetasizer® Software (version 7.11) was used for data acquisition and analysis.

The siRNA encapsulation efficiency and practical loading of the LPNs were measured as previously reported (32). Briefly, a volume of 25 μ l LPN dispersion was mixed with 200 μ l CHCl_3 and vortexed for 2 min. Thereafter, a volume of 475 μ l HD-solution was added to the sample and vortexed for 1 min to ensure complete extraction of siRNA into the aqueous phase. The two phases were separated by centrifugation for 12 min at 4°C and 22000 g. The supernatant (50 μ l) was transferred and diluted with 950 μ l HD-solution. To all samples, the RiboGreen® RNA reagent (1.5 μ l RiboGreen® RNA reagent added to 3 ml TE buffer) was added. Subsequently, the concentration of siRNA was measured by using a fluorescence plate reader (FLUOstar OPTIMA, BMG Labtech, DE) with excitation and emission wavelengths of 485 nm and 520 nm, respectively. The siRNA encapsulation efficiency and practical loading were calculated according to Eq. 1 and Eq. 2:

$$\text{Encapsulation efficiency} = \frac{\text{Amount of encapsulated siRNA}}{\text{Total amount of added siRNA}} \times 100 \quad (1)$$

$$\text{Practical loading} = \frac{\text{Amount of encapsulated siRNA}}{\text{Total weight of nanoparticles}} \times 100 \quad (2)$$

3.3. SPRAY DRYING OF LPNs INTO NANOCOMPOSITE MICROPARTICLES

Dry powder particles were manufactured by spray drying the formulations using a co-current Büchi B-290 mini spray dryer (Büchi Labortechnik, Flawil, Switzerland). The formulations for spray drying were prepared with a loading of 5% (w/w), a solid concentration of 25 mg/ml and a binary mixture of stabilizing excipients, *i.e.* trehalose (T) and dextran (D), at different weight ratios. The used weight ratios of T/D were 50:50, 40:60, 30:70, 20:80, 10:90 and 5:95, respectively. The samples were dispersed in DEPC-water to a total volume of 10 ml. Nitrogen was used as atomizing gas, and the spray dryer was equipped with a nozzle atomizer with an orifice diameter of 0.7 mm. A high-performance cyclone (Büchi Labortechnik) was used to separate the dry powder particles from the airstream by centrifugal forces. The following spray drying settings were used: an outlet temperature of 50 °C, an aspirator capacity of 90%, a feed flow rate of 0.7 ml/min and an atomizing airflow of 742 l/h (49).

3.4. POWDER YIELD

The powder yield was measured as the percentage of powder collected in the collection vessel after spray drying relative to the starting material. It was determined as the difference in weight of the collection vessel before and after spray drying. This difference was divided by the total solid content of the spray-dried dispersions, *i.e.* 25 mg/ml (Equation 3).

$$\text{Yield}\% = \frac{\text{collection vessel after drying (mg)} - \text{collection vessel before drying (mg)}}{\text{Total solid content (mg)}} \times 100 \quad (3)$$

3.5. REDISPERSIBILITY

To evaluate the redispersion of the nanocomposite microparticles into a homogenous suspension of LPNs, a volume of carbohydrate solution (T/D) or DEPC-water was added to the powder, providing a solid concentration identical to the solid concentration before spray drying (*i.e.* 7.5 mg/ml LPNs). The mixture was bath-sonicated until all powder was completely dissolved. The *z*-average, PDI and zeta potential were measured as described above. For analysis, the reconstituted LPNs were diluted 40 times with DEPC-water (25 µl reconstituted LPNs + 975 µl DEPC-water). The siRNA encapsulation efficiency of the LPNs after reconstitution was determined as described above (3.2 Nanoparticle preparation and physicochemical characterization).

3.6. SOLID STATE CHARACTERIZATION

The aerodynamic particle size of the spray-dried powders was examined by using an Aerodynamic Particle Sizer (APS) Spectrophotometer 3321 equipped with a small-scale powder disperser (TSI, Shoreview, MN, USA) used to generate the aerosol as previously described (24). The aerodynamic particle size is reported as the mass median aerodynamic diameter (MMAD) in the following text.

The residual moisture content of the powders was investigated by thermogravimetric analysis (TGA). A Discovery TGA 550 (Perkin Elmer, Waltham, Massachusetts, USA) was used with nitrogen purging. Approximately 10 mg of the powder samples was loaded onto the platinum sample pans of the TGA and heated at a constant rate of 30 °C/min up to 300°C. The weight loss in % caused by evaporations was calculated by using the TRIOS software (version 4.3) and defined as the moisture content.

The surface morphology of the spray-dried powders was determined by scanning electron microscopy (SEM) using a Hitachi TM3030 SEM (Krefeld, Germany). The operation settings were used as previously described (82). Briefly, an accelerating voltage of 15 kV, a working distance of 5.8 mm and an emission current of 53.5 A, were used. The examined powder was deposited onto a SEM stub covered with double-adhesive carbon tape and was sputter-coated with gold at a sputter current supply of 30 mA for 30 s using a Cressington Sputter Coater 108 auto (Watford, England). The magnification was set at 2000x to acquire the images and the scanning speed was set at low to optimize the resolution.

The X-ray powder diffraction (XRPD) patterns were investigated with a PANalytical X-ray diffractometer of the XPERT PRO type with a PW 3050/60 generator and a PIXcel Detector (PANalytical, Almelo, The Netherlands). The X-ray diffractometer was operated at an accelerating voltage of 30 kV and an anode current of 40 mA. The samples were placed onto an aluminum sample tray and exposed to a CuK α radiation source at diffraction angles ($2-\theta$) from 5° to 35° in a step mode using a step size of 0.02° of $2-\theta$ and a collection time of 96 s per step. For data analysis, the X'Pert Data Collector software for automatic powder diffraction version 2.2i was used (PANalytical).

3.7. AEROSOL GENERATION IN PRECISEINHALE™

To generate the aerosols, the PI aerosol generator was used as described previously (77, 83). Briefly, the DustGun aerosol generator of the PI system consisted of a powder chamber with an exit nozzle that was connected to the holding chamber and an exposure line exiting the holding chamber. The aerosol generator was connected to a vacuum pump for regulation of the aerosol flow rate, a pressure chamber with an adjustable volume of compressed gas to deagglomerate cohesive powders to aerosols, and a computerized control system. Settings and materials were used as reported previously (49). In short, an impactor nozzle, which is suitable for more cohesive and dense powders, was used. The aerosol generation pressure was set to 130 bar, the aerosol flow rate was 66 ml/min and a main valve reset pressure of 65 bar was used. In addition, a pre-exposure aerosol mixing period of 0.6 s and a plunger displacement of 4.5 mm were used. During aerosol generation, 1 mg test powder was loaded into the retractable powder chamber bottom, inserted into the PI, and secured. The exposure time of the powder was set to 350 s.

The aim of aerosol generation was to investigate the flyability of the powders. This was measured as the Casella maximum concentration (C_{max}). For each dry powder formulation, C_{max} was measured five times by CEL 712 Microdust Pro Real-time Dust Monitor, which is a data logging instrument that displays real-time graphical dust levels (Casella, Bedford, UK)(49).

The PI aerosol yield was determined as the percentage of the dry powders that was deposited on the end filter after PI exposure. The weight difference of the end filter before and after PI exposure of the dry powder formulation was divided by the weight of the loaded powder in the powder chamber (Equation 4).

$$\text{Aerosol yield\%} = \frac{\text{End filter after PI exposure (mg)} - \text{End filter before PI exposure (mg)}}{\text{Loaded powder in the powder chamber (mg)}} \times 100 \quad (4)$$

3.8. PARTICLE SIZE DISTRIBUTION

The aerodynamic particle size distribution (PSD) of the aerosols was analyzed by cascade impaction analysis using a nine-stage Marple Cascade Impactor (MSP corporation, Shoreview, MN, USA). The Marple Cascade Impactor was connected to the PreciseInhale™ and the aerosol, generated at a generation pressure of 130 bar, a reset pressure of 65 bar and a plunger displacement of 4.5 mm, was drawn through the impactor at a flow rate of 2 l/min. Based on their sizes, the particles were captured by impaction on the cascade impactor stages. Subsequently, the PSD was calculated from the amount of drug substance deposited onto each of the impactor stage filters. The measurements were performed in triplicate.

3.9. STATISTICS

The measurements of the physicochemical characteristics and the aerodynamic particle size were performed in triplicate, unless otherwise stated. Values are given as mean \pm standard deviation (SD). C_{\max} between formulations were compared by one-way ANOVA followed by Tukey's multiple comparisons test. Statistical analysis of the data was performed using the GraphPad Prism 8 (Graphpad Software Inc, La Jolla, CA, USA). A value of $p < 0.05$ was considered significant. Statistically significant differences were displayed as $p < 0.05$ (*), $p < 0.01$ (**), and $p < 0.001$ (***)

4. RESULTS

4.1. PREPARATION AND CHARACTERIZATION OF TNF- α siRNA-LOADED LPNs

The TNF- α siRNA-loaded LPNs were prepared by using the DESE method as described previously (32). The LPNs consisted of an L₅ content relative to the total solid content (*i.e.* L₅ + PLGA) of 15% (w/w), and the L₅:siRNA ratio was kept constant at 15:1 (w/w). This composition was selected based on previous experiments (10, 82). In addition, the composition of the formulation and the preparation method were kept constant throughout the project. The *z*-average of the LPNs was 204.6 nm with a PDI of 0.101, and the zeta potential was 16.9 mV (Table 4.1). These results are similar to previously reported data (82). The PDI value suggests a relatively monodisperse particle size distribution, which is also apparent from the intensity-based particle size distribution (Figure 4.1). An siRNA encapsulation efficiency of 68.2% and a loading of 6.80 μ g siRNA/mg LPNs are well in accordance with previously published data (82).

Table 4.1 Physicochemical properties of TNF- α siRNA-loaded LPNs. Data represent mean values \pm SD (n=8).

<i>z</i> -average (nm)	PDI	Zeta potential (mV)	Encapsulation efficiency (%)	Loading (μ g siRNA/mg LPNs)
204.6 \pm 9.9	0.101 \pm 0.019	16.9 \pm 6.4	68.2 \pm 12.7	6.80 \pm 1.26

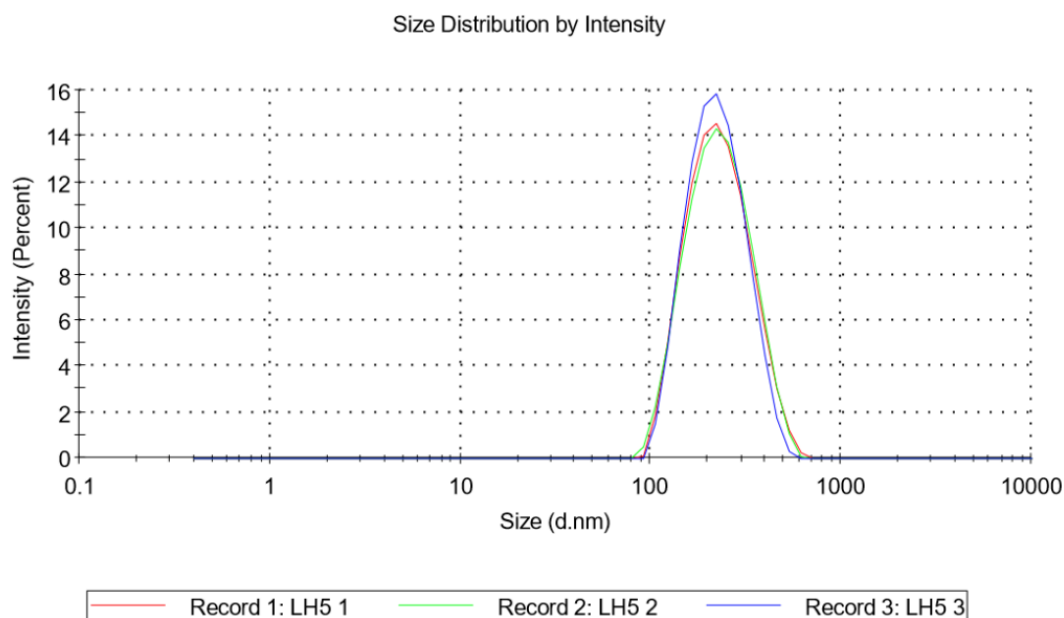


Figure 4.1: Graph showing representative intensity-based hydrodynamic size distributions of LPNs obtained by dynamic light scattering using a Zetasizer. LH5 refers to LPN-formulation 5. The red, green and blue curves represent three different measurements of the same formulation.

4.2. SPRAY DRYING INFLUENCES THE PHYSICOCHEMICAL PROPERTIES OF THE TNF- α siRNA-LOADED LPNs

The TNF- α siRNA-loaded LPNs were spray-dried to manufacture powder-based solid dosage forms suitable for pulmonary delivery. Different ratios of trehalose/dextran were used as carbohydrate excipient. Furthermore, the spray-dried samples displayed a total volume of 10 ml, a solid concentration of 25 mg/ml and an LPN loading of 5% (w/w). The spray drying process parameters were kept constant.

The LPNs were spray dried in the presence of five different ratios of trehalose and dextran, as stabilizing excipients, to study the effect on the aerodynamic properties and the powder flyability in PI. Moreover, the effects on the physicochemical properties of the LPNs after spray drying into nanocomposite microparticles were investigated to ensure preservation of the integrity of the LPNs after spray drying. The z -average, PDI and zeta potential were first determined after reconstitution of the dry powder in a carbohydrate solution (T/D 40:60, Table 4.2). The z -average of spray-dried, reconstituted LPN-T/D formulations 50:50, 40:60, 30:70, and 20:80 were 516.6, 681.8, 724.5, and 1053.1 nm, respectively, with PDIs of 0.187, 0.272, 0.499, and 0.801, respectively. The zeta potential ranged from 10.1 mV to 16.8 mV. These data were compared to the physicochemical properties before spray drying (Table 4.2). The increase in size ratio (*i.e.* the z -average after spray drying relative to the z -average before spray drying) suggests an increase in particle size after spray drying. Likewise, an increase in PDI was observed from 0.101 to approximately 0.400, which indicates that the LPN size distribution was more polydisperse after reconstitution.

Table 4.2: Physicochemical properties of spray-dried, reconstituted formulations of TNF- α siRNA-loaded LPNs (LPN-T/D) in carbohydrate solution. LPN-T/D ratios were 50:50 (n=1), 40:60 (n=2), 30:70 (n=2), and 20:80 (n=1). Data represent mean values.

Formulation	z -average (nm)	PDI	Zeta potential (mV)	Size ratio
LPN-T/D 50:50	516.6	0.187	16.8	2.52
LPN-T/D 40:60	681.8	0.272	10.1	3.33
LPN-T/D 30:70	724.5	0.499	14.1	3.54
LPN-T/D 20:80	1053.1	0.801	4.1	5.15

The increase in size might be due to a higher viscosity of the redispersion medium caused by mistakenly using a carbohydrate solution for the reconstitution. Hence, the experiments were repeated by reconstituting the spray-dried powders in DEPC-water, and the physicochemical properties of the spray-dried formulations,

reconstituted in both carbohydrate solution and DEPC-water, were compared (Table 4.3). The *z*-average of the spray-dried LPNs reconstituted in carbohydrate solution was between 319.2 and 494.7 nm, while the *z*-average of the same LPN formulations reconstituted in DEPC-water ranged from 306.6 to 393.6 nm with a PDI of 0.280 to 0.375. The size ratio suggests a smaller increase in particle size after reconstitution of the powder in DEPC-water compared to reconstitution in carbohydrate solution (Table 4.3). A small increase in zeta potential was observed from approximately 8 mV after reconstitution in carbohydrate solution to approximately 16 mV after reconstitution in DEPC-water.

Table 4.3: Physicochemical properties of spray-dried, reconstituted LPN-T/D in carbohydrate solution (LPN-T/D) 20:80 (n=1), 10:90 (n=1), and 5:95 (n=1) and of spray-dried, reconstituted LPN-T/D in DEPC-water (LPN-T/D) 20:80 (n=1), 10:90 (n=1), and 5:95 (n=1). Data represent mean values.

Formulation	Reconstituted in carbohydrate solution (T/D 40:60)				Reconstituted in DEPC-water			
	<i>z</i> -average (nm)	PDI	Zeta potential (mV)	Size ratio	<i>z</i> -average (nm)	PDI	Zeta potential (mV)	Size ratio
LPN-T/D 20:80	494.7	0.561	5.92	2.42	393.6	0.375	16.8	1.92
LPN-T/D 10:90	319.2	0.318	11.9	1.56	306.6	0.280	18.8	1.50
LPN-T/D 5:95	402.9	0.406	6.76	1.97	364.4	0.285	12.1	1.78

Table 4.4: Encapsulation efficiencies of spray-dried, reconstituted formulations of TNF- α siRNA-loaded LPNs (LPN-T/D) 50:50, 40:60, 30:70, 20:80, 10:90, and 5:95. Data represent the value of one measurement.

Formulation	Encapsulation efficiency (%) after spray drying	
	Experiment 1 ^a	Experiment 2 ^b
LPN-T/D 50:50	22.5	
LPN-T/D 40:60	39.8	
LPN-T/D 30:70	25.0	
LPN-T/D 20:80	31.1	52.6
LPN-T/D 10:90		51.0
LPN-T/D 5:95		60.4

^a Experiment 1 was performed after reconstitution of the spray-dried LPNs in carbohydrate solution (T/D).

^b Experiment 2 was performed after reconstitution of the spray-dried LPNs in DEPC-water.

The encapsulation efficiency of the spray-dried LPN formulations was determined after reconstitution. During the first measurements of the encapsulation efficiency, the reconstitution of the powder particles was performed using carbohydrate solution (T/D). The encapsulation efficiencies of the LPN-T/D formulations 50:50, 40:60, 30:70, and 20:80 were 22.5, 39.8, 25.0, and 31.1%, respectively (Table 4.4). A second measurement of the encapsulation efficiency was performed for spray-dried LPNs reconstituted in DEPC-water. The values for the encapsulation efficiency were 52.6, 51.0, and 60.4% for the LPN-T/D formulations 20:80, 10:90, and 5:95, respectively (Table 4.4).

4.3. POWDER YIELD AND AERODYNAMIC PROPERTIES OF THE SPRAY-DRIED LPNs

The dry powder yield (%) for the LPNs spray-dried in the presence of different ratios of the sugars (T/D) (*i.e.* 50:50, 40:60, 30:70, 20:80, 10:90, and 5:95, w/w) ranged from 46.7% to 78.9% (Table 4.5). According to previous experiments, the yield should be higher than 40% for the spray drying process to be economic feasible (82). The MMAD was determined for the LPN-T/D spray-dried formulations 50:50, 40:60, 30:70, 20:80, 10:90, and 5:95 (Table 4.5). The MMAD values were 3.25, 4.35, 3.67, 3.61, 4.35, and 4.13 μm , respectively, which suggests that the powders are suitable for deposition into the deep lungs after pulmonary administration (41). Furthermore, the use of different ratios of trehalose/dextran was not causing any major differences in the MMAD. The residual moisture content, determined by using TGA, showed that the powders displayed a water content between 1.60 and 6.53% (Table 4.5).

Table 4.5: Dry powder yield (%), mass mean aerodynamic diameter (MMAD) and moisture content of spray-dried, TNF- α siRNA-loaded LPNs (LPN-T/D) 50:50 (n=2), 40:60 (n=2), 30:70 (n=2), 20:80 (n=2), 10:90 (n=1), and 5:95 (n=1). Data represent mean values.

Formulation	Dry powder yield (%)	MMAD (μm)	Moisture content (%)
LPN-T/D 50:50	63.5	3.25	3.26
LPN-T/D 40:60	53.5	4.35	6.53
LPN-T/D 30:70	46.7	3.67	5.21
LPN-T/D 20:80	63.8	3.61	1.60
LPN-T/D 10:90	78.9	4.35	
LPN-T/D 5:95	70.8	4.13	

4.4. SURFACE MORPHOLOGY OF THE SPRAY-DRIED LPNs

Morphological analysis of the spray-dried LPN formulations using SEM showed that LPN-T/D 50:50, 40:60, 30:70, and 20:80 displayed smooth and spherical microparticles (Figure 4.2A, B, C, and D). However, the SEM analysis of LPN-T/D 10:90 and 5:95 showed slightly corrugated particles (Figure 4.2E and F). Furthermore, SEM image analysis confirmed that the powders consisted of particles with an MMAD smaller than 5 μm . SEM images of LPN-T/D 20:80, 10:90, and 5:95 were taken for a more detailed investigation of the surface morphology (Figure 4.3). These images showed a slightly corrugated surface for LPN-T/D 10:90 and 5:95 (Figure 4.3B and C), whereas the surface of LPN-T/D 20:80 appeared more smooth (Figure 4.3A).

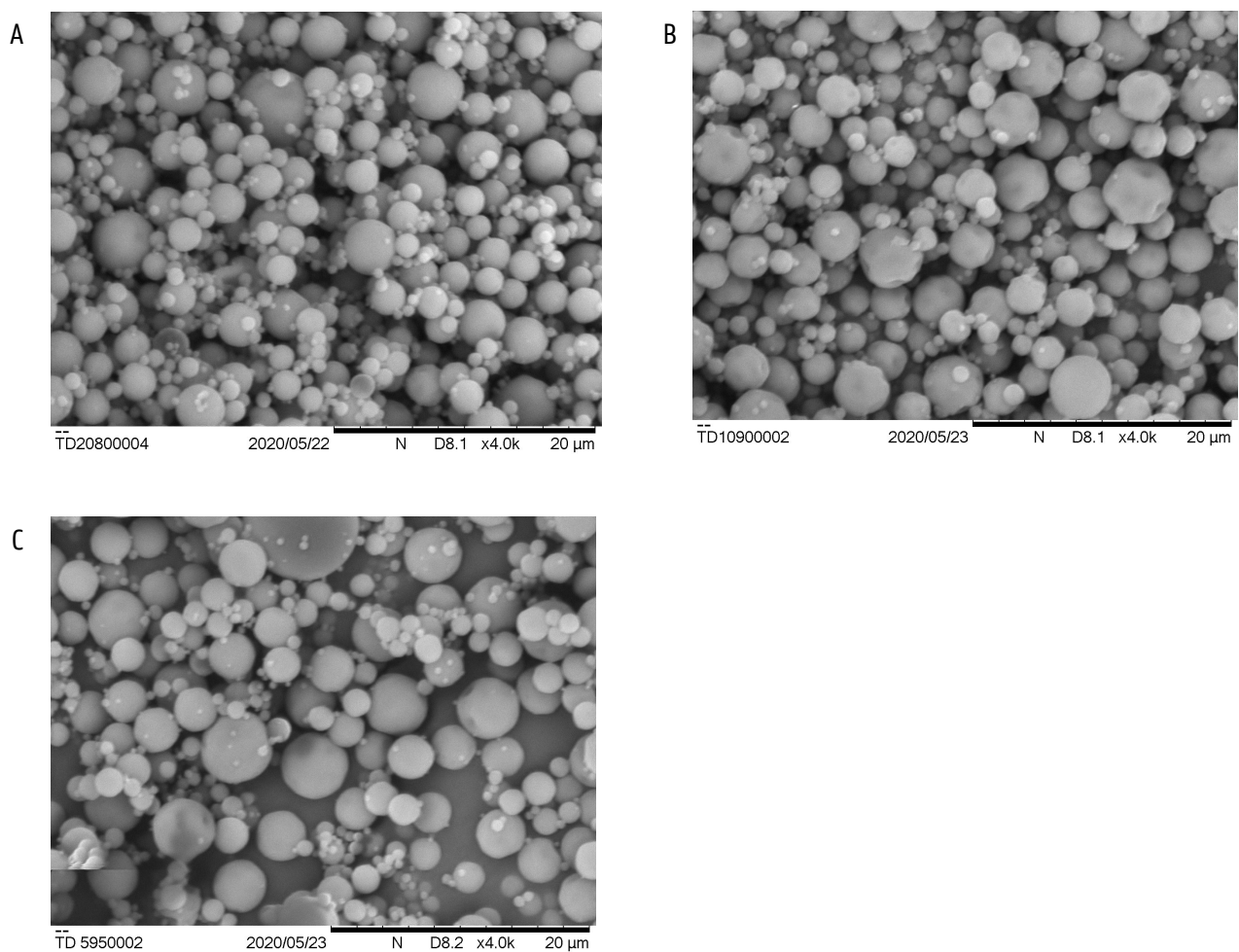


Figure 4.3: Representative scanning electron microscopy images of the LPN-trehalose/dextran (LPN-T/D) powder formulations, microscopic magnification 4000x. A) LPN-T/D 20:80, B) LPN-T/D 10:90, C) LPN-T/D 5:95.

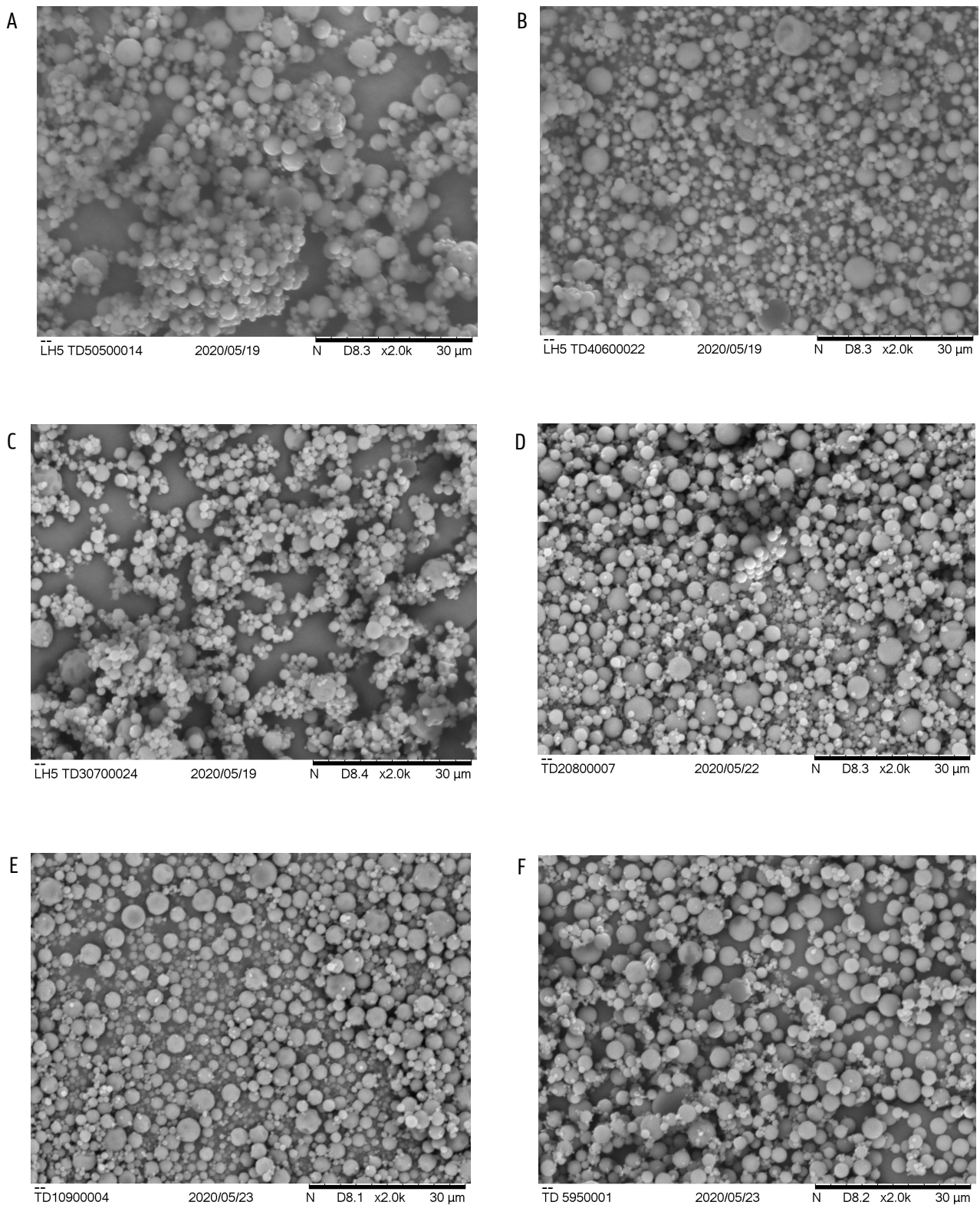


Figure 4.2: Representative scanning electron microscopy images of the LPN-trehalose/dextran (LPN-T/D) powder formulations, microscopic magnification 2000x. A) LPN-T/D 50:50, B) LPN-T/D 40:60, C) LPN-T/D 30:70, D) LPN-T/D 20:80, E) LPN-T/D 10:90, and F) LPN-T/D 5:95.

4.5. FLYABILITY OF NANOCOMPOSITE MICROPARTICLES

The spray-dried LPN formulations with T/D ratios 50:50, 40:60, 30:70, and 20:80 were tested in PI. The maximum concentration in Casella (C_{max}) (mg/l) was measured, which reflects the powder flyability in the PI device. The applied PI parameters were a generation pressure of 130 bar, a reset pressure of 65 bar, and a plunger displacement of 4.5 mm. Further, a flow rate of 400 ml/min, a holding chamber of 310 ml and an exposure time of 90 s were used. The formulation containing the lowest dextran concentration (*i.e.* LPN-T/D 50:50), displayed the lowest C_{max} , which was 0.45 mg/l (Figure 4.4A). An increase in the C_{max} could be observed at increasing concentration of dextran in the formulation. LPN-T/D 20:80 had a C_{max} of 0.87 mg/l (Figure 4.4A). LPN-T/D 20:80 and 30:70 had a statistically significant higher C_{max} than LPN-T/D 40:60 and LPN-T/D 50:50.

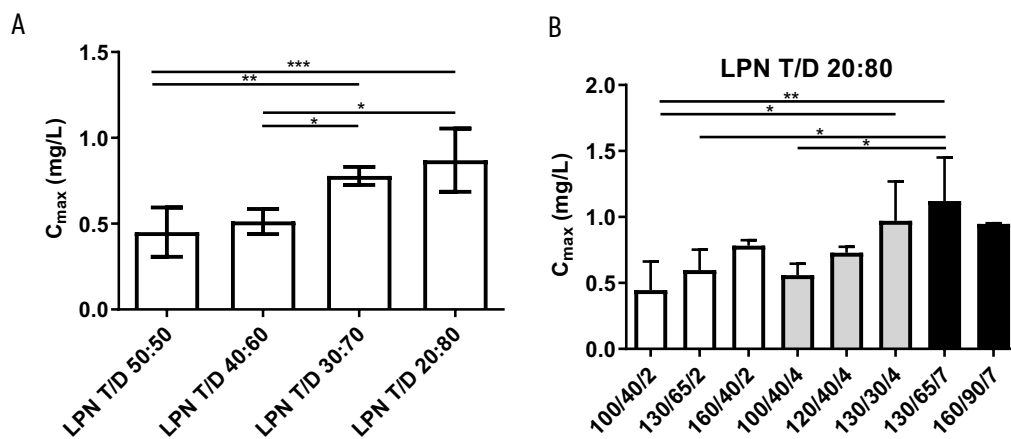


Figure 4.4: A) C_{max} (mg/l) of LPN-T/D 50:50, 40:60, 30:70, and 20:80 measured in PI. Data represent mean \pm SD. One-way ANOVA followed by Tukey's multiple comparisons test was used as statistical analysis to compare C_{max} between the formulations. A value of $p < 0.05$ was considered significant, $p < 0.05$ (*), $p < 0.01$ (**), $p < 0.001$ (***). B) C_{max} of LPN-T/D 20:80 was measured using different PI settings: 100/40/2, 130/65/2, 160/40/2, 100/40/4, 120/40/4, 130/30/4, 130/65/7, and 160/90/7 which represents generation pressure, reset pressure, and plunger displacement respectively. Data represent mean \pm SD. One-way ANOVA followed by Tukey's multiple comparisons test was used as statistical analysis. A value of $p < 0.05$ was considered significant, $p < 0.05$ (*), $p < 0.01$ (**), $p < 0.001$ (***).

The spray-dried formulation LPN-T/D 20:80 was used to optimize the aerosol exposure settings. Eight different settings were tested, (i) generation pressure = 100 bar, reset pressure = 40 bar, and plunger displacement = 2 mm, (ii) generation pressure = 130 bar, reset pressure = 65 bar, and plunger displacement = 2 mm, (iii) generation pressure = 160 bar, reset pressure = 40 bar, and plunger displacement = 2 mm; (iv) generation pressure = 100 bar, reset pressure = 40 bar, and plunger displacement = 4 mm, (v) generation

pressure = 120 bar, reset pressure = 40 bar, and plunger displacement = 4 mm, (vi) generation pressure = 130 bar, reset pressure = 30 bar, and plunger displacement = 4 mm, (vii) generation pressure = 130 bar, reset pressure = 65 bar, and plunger displacement = 7 mm, (viii) generation pressure = 160 bar, reset pressure = 90 bar, and plunger displacement = 7 mm. The highest C_{max} of 1.12 mg/l was obtained for the PI settings: generation pressure = 130, reset pressure = 65, and plunger displacement = 7 mm (Figure 4.4B).

5. DISCUSSION

The final goal of this project was to optimize the aerosolization properties of a powder-based solid dosage form of TNF- α siRNA-loaded LPNs suitable for pulmonary delivery by optimizing the ratio of the carbohydrate excipients, *i.e.* trehalose and dextran, used to spray dry the LPN dispersions. Previous studies from the group provided optimized siRNA-loaded L₅-modified LPNs with safe and efficient intracellular delivery of siRNA (28). Furthermore, the factors of importance for spray drying of siRNA-loaded LPNs were identified and the influence on the dry powders was evaluated (82, 84). The determined optimal factors for spray drying (*i.e.* an LPN loading of 5% (w/w), a solid concentration of 25 mg/ml, and an outlet temperature of 50 °C) were used throughout this project. In addition, optimization of the aerodynamic properties and flyability of cationic adjuvant formulation O1 (CAF01) liposomes, which were spray-dried into dry powder formulations, has been performed (49). The carbohydrate excipients trehalose and dextran in a ratio of 30:70 provided the most promising formulation after spray drying of CAF01 in terms of physicochemical characterization and flyability in PI (Master Thesis, Guillermo Cano, unpublished data).

In this project, dry powder formulations containing TNF- α siRNA-loaded LPNs, were optimized. The LPN dispersions were spray dried using different ratios of trehalose/dextran as stabilizing excipient. Subsequently, the physicochemical properties of the formulations *i.e.* particle size, zeta potential, and encapsulation efficiency before and after spray drying were determined. Moreover, to characterize the powder properties, the solid state characterization was performed *e.g.*, MMAD, residual moisture content, surface morphology, and flyability.

The physicochemical characterization performed on the prepared, liquid LPN formulations, showed that the size and PDI of the LPNs were in accordance to previous reported data (10). Controlling the size of the nanoparticles during the spray drying process is necessary as quality control to ensure the structural integrity of the LPNs, which provides safe and efficient delivery of siRNA. Therefore, the nanoparticle size was determined after spray drying of the LPNs into nanocomposite microparticles.

To measure the *z*-average, PDI and zeta potential of the spray-dried powders using dynamic light scattering, reconstitution into a homogenous suspension of LPNs was necessary. Due to a misunderstanding, the spray-dried powders were first reconstituted in a carbohydrate solution (T/D 40:60), providing a solid concentration identical as before spray drying. When the physicochemical properties of the liquid formulations and the spray-dried formulations, reconstituted in carbohydrate solution, were compared, an increase in size and PDI after spray drying was present. Due to reconstitution in sugar solution, an increase in viscosity of the

redispersion was observed. Hence, this might be a possible explanation for the increase in size of the LPNs because viscosity has an influence on the measurements performed by dynamic light scattering. More specifically, a higher viscosity of the redispersion causes slower diffusion of the LPNs in the suspension, resulting in a higher particle size measured by dynamic light scattering.

To confirm this hypothesis, the physicochemical properties of the spray-dried, reconstituted LPNs in carbohydrate solution were compared to the physicochemical properties after reconstitution in DEPC-water. The results showed a decrease in particle size after reconstitution of the dry powder in DEPC-water compared to reconstitution of the same powder in carbohydrate solution. This suggests that the use of a carbohydrate solution, as solvent for performing the reconstitution, has an influence on the particle size measured by dynamic light scattering. Therefore, the particle size of the LPNs in the redispersion should preferably be determined by using DEPC-water for the reconstitution.

The results of the physicochemical characterization of the spray-dried LPN formulations, after reconstitution in DEPC-water, display a slight increase in particle size compared to the liquid LPN formulations before spray drying. This could indicate that some fusions or aggregations between the nanoparticles have occurred. Further experiments are needed to investigate this hypothesis. For example, cryo-transmission electron microscopy could be used to study the morphology of the LPNs before and after spray drying. The nanoparticle size after spray drying should preferably be equal to the particle size before spray drying, resulting in a size ratio with a value close to one, to preserve the structural integrity of the LPNs. Further optimization of the excipients and/or the process parameters during spray drying might be needed to improve the size ratio.

The determination of the encapsulation efficiency of the spray-dried, reconstituted formulations was performed twice. The results of the first experiment showed a decrease in encapsulation efficiency after spray drying compared to the encapsulation efficiency of siRNA in the LPN dispersions before spray drying. This might be due to the difficulties experienced while redispersing the formulations. The powders were relatively hydrophobic, providing a higher risk of powder agglomerations, which were not fully redispersed. Therefore, the amount of encapsulated siRNA is not representative, and due to the dilutions performed during the measurement of the encapsulation efficiency, a small error is magnified. Hence, a second experiment was performed, and no major decrease in encapsulation efficiency was found. This could be due to improved redispersion of the powder particles, which was observed during the second experiment. Therefore, we could hypothesize that the quality of the redispersion has an influence on the encapsulation efficiency. However, more

measurements are needed to draw any conclusions. Furthermore, during the first experiment, spray-dried LPNs were reconstituted in carbohydrate solution, whereas DEPC-water was used for reconstitution of spray-dried LPNs in the second experiment. Similarly, further investigation of the influence of these parameters on the encapsulation efficiency is needed by repeating the measurements.

It may be possible that the investigated excipient mixture trehalose/dextran is not optimal for the preservation of the physicochemical characteristics of the nanoparticles during spray drying. Hence, other stabilizing excipients can be investigated for further optimization of the nanoparticle characteristics and the powder.

The dry powder yield obtained after spray drying of the LPN formulations should be as high as possible to ensure a cost-effective process. In a previous study from the group, which investigated the factors of importance for spray drying of siRNA-loaded LPNs, a target for the yield was set to be higher than 40% (82). After calculation of the dry powder yield obtained in this project, all formulations reached a yield higher than 40%. Hence, we can conclude that the used spray drying process can be considered as cost-effective.

The MMAD of the produced powder particles is one of the most important factors to control the deposition site of the particles in the lungs. In the upper respiratory tract, pulmonary administered particles are subjected to mucociliary clearance and phagocytosis (38). To avoid these natural defense mechanisms, deposition into the deep lungs is needed. Particles with an MMAD between 1 and 5 μm are most appropriate to target this site of deposition (41). Smaller particles with an MMAD below 1 μm have a high probability of being exhaled, whereas larger particles (*i.e.* MMAD > 5 μm) are deposited in the upper airways and oropharynx, where they will be expectorated or swallowed. We found that the MMAD of the obtained nanocomposite microparticles ranged from 3 to 4.5 μm , rendering them suitable for deposition in the lower respiratory tract after pulmonary administration. Furthermore, the use of different ratios of trehalose and dextran as carbohydrate excipients during spray drying did not display a major influence on the MMAD of the spray-dried powder particles. However, it has been reported previously that particles with an MMAD below 3 μm display a higher powder flyability (49). Regarding the available literature, mainly two process parameters have an influence on a further decrease of the MMAD, *i.e.* the atomization airflow and the feedstock concentration (85). Due to an increase of the atomization airflow, a larger energy input is applied to atomize the feed dispersion into smaller droplets, which consequently results in a reduced particle size (85). On the other hand, the feedstock concentration has a positive effect on the particle size, as the MMAD increases with a higher concentration of the feed formulation (24, 86). This is thought to be

caused by an increase in solid content in each droplet, assuming that one droplet dries to one particle, which eventually results in an increased particle size. Hence, these two parameters could be further optimized to obtain a decrease in the MMAD, which could possibly allow for further improvement of the powder flyability.

In addition to the MMAD, the residual moisture content is another parameter that can influence the flyability of the powders. A lower moisture content will decrease the cohesion between the powder particles and thereby improve the flyability of the powders through the respiratory tract (24). Moreover, a high moisture content has a negative effect on the stability of the powders. Specifically, an increase in moisture provides a decrease in T_g of the sugar excipient, used to stabilize the nanoparticles, because water acts as a plasticizer (54). As the T_g of the sugar excipient decreases below the storage temperature, the sugar alters from an amorphous, glassy matrix to a rubbery state. Consequently, the molecular mobility increases, leading to an increase in degradation rate of the powder particles. It has been described in the literature that the type of carbohydrate excipient used for spray drying can influence the residual moisture content (51). Unfortunately, it was not possible to generate data of the residual moisture content for the LPN formulations spray dried with ratios T/D 10:90 and 5:95 due to lack of time caused by the general COVID-19 lockdown in Denmark. Furthermore, the obtained results are based on only one measurement, rendering it impossible to draw a solid conclusion about the influence of the stabilizing excipients T/D in different ratios on the residual moisture content, and consequently on the flyability of the produced powders. However, according to the literature, trehalose is highly hygroscopic and thereby responsible for a higher moisture content in the powder formulations (60). Therefore, it can be assumed that a lower residual moisture can be achieved as the concentration of trehalose used as stabilizing excipient, decreases. In order to confirm this hypothesis, more data is needed for each ratio of T/D used during spray drying of the LPNs.

The aerosolization properties of the spray-dried powders can also be influenced by the surface morphology of the spray-dried particles. It has been shown that particles with a corrugated surface display a higher aerosol performance of the spray-dried powders, compared to smooth particles (87-89). Due to the corrugated surface of the particles, there is a decrease in the total surface area accessible for particle interaction and an increase in distance between the particles (89). Consequently, the cohesion between the particles is reduced, which can explain the improved flyability of the powder. In addition, a relatively small degree of surface corrugation is sufficient to obtain a considerable improvement in the aerosolization properties of the powder (88). In this project, mainly the powder particles spray-dried by using the stabilizing excipients T/D in ratio 10:90 and 5:95, tend to have a slightly corrugated surface. However, no data are available about the flyability of these powders.

Consequently, no conclusions can be made about the influence of the surface morphology on the flyability in this project. A previous study of the group showed that the inclusion of dextran as stabilizing excipient affected the surface morphology of spray-dried CAF01 liposomes and consequently resulted in a higher C_{max} (49). To investigate whether this finding is also applicable for spray drying of LPNs, generation of more data about both surface morphology and flyability of formulations spray dried at different ratios T/D, is needed. Nevertheless, the images from the SEM analysis confirm that all the LPN formulations, spray-dried at different ratios T/D, have an MMAD smaller than 5 μm , which allows for deep lung deposition of the powders after pulmonary administration.

The use of the disaccharide trehalose as stabilizer during spray drying, provides a good coating of the nanoparticles according to the water replacement theory. On the other hand, the polysaccharide dextran has a higher T_g compared to trehalose, which favors the vitrification theory. However, due to the large size and rigidity of dextran, this sugar is not able to provide a proper coating of the nanoparticle due to steric hindrance (55). Achieving a good particle coating and a high T_g is difficult using a single saccharide as stabilizing excipient (62). Therefore, the combination of trehalose and dextran can provide an increase in T_g and a better coating of the nanoparticles, resulting in improvement of the stability of the formulation (55, 57, 62). It has been described in the literature that a mixture of trehalose and dextran, acting as stabilizers, improves the stability of the powder formulations both for freeze-dried proteins and for a spray freeze-dried influenza vaccine (62, 90). Furthermore, the influenza vaccine powder particles had an aerodynamic diameter suitable for inhalation. In this project, the formulations were spray-dried at different ratios of trehalose and dextran. The flyability of the resulting powders was tested using the PI system. The results showed that with an increasing concentration of dextran as stabilizer, the flyability increased accordingly. This suggests that dextran is associated with improved aerosolization properties of the spray-dried powders. The increase in concentration of dextran can provide an increase in T_g of the dried formulations and further improve the rigidity of the structures. Consequently, a better coating and stability of the LPNs can be achieved, which could be associated with the higher C_{max} measured in PI. However, more experiments are needed to investigate the influence of dextran on the powder properties. For example, particle density, influenced by the use of a carbohydrate excipient, could play a role in altering the aerosolization properties of the spray-dried formulations (46). Therefore, gas pycnometry could be used to study the impact of the particle density on the flyability of the powders (91).

Mainly three settings in PI (*i.e.* the generation pressure, the reset pressure, and the plunger displacement) can influence the aerosolization properties of the powder particles. By controlling these settings, the ejected

volume and the C_{max} of the powders can be regulated. In order to obtain a further improvement of C_{max} , we used the powder formulation LPN-T/D 20:80 as a representative parameter to determine the most optimal PI settings. The results showed that a generation pressure of 130 bar, a reset pressure of 65 bar, and a plunger displacement of 7 mm, were the PI settings which provided the highest C_{max} for the spray-dried LPN formulation LPN-T/D 20:80.

To determine the most promising powder formulation based on aerodynamic characteristics and aerosol performance, more data is needed for LPN-T/D 10:90 and 5:95. The experiments for these ratios were not performed due to the general COVID-19 lockdown in Denmark. Furthermore, the experiments should be repeated to ensure representative results.

For further characterization of the most optimal LPN-T/D ratio, XRPD analyses can be performed to determine the solid form of the carbohydrate excipients used in the spray-dried LPNs. It is well-known that trehalose provides an X-ray amorphous pattern (53, 92), and amorphous structures allow for better stabilization properties. If the carbohydrate mixture trehalose/dextran shows an amorphous pattern after XRPD analyses of the spray-dried LPNs, it can be considered as an adequate stabilizing excipient for spray drying. In a previous study from the group, XRPD analysis showed an amorphous pattern for CAF01 liposomes spray dried using trehalose/dextran ratio 30:70 as stabilizing excipient (49). Furthermore, the aerosol yield and PSD of the most optimal ratio can be measured in the PI system. A higher aerosol yield can provide a higher amount of powder that will be deposited in the lung of the animal during *in vivo* exposure. Hence, it is important to obtain powders with an acceptable aerosol yield, rendering them suitable for future pre-clinical studies.

6. CONCLUSION AND FUTURE PERSPECTIVES

The results of the physicochemical properties of the LPNs, after reconstitution of the spray-dried powder, demonstrate a slight increase in nanoparticle size. Further experiments are required to investigate if the LPNs can be considered as sufficiently stable for safe and efficient delivery of siRNA to the target cells. In addition, further optimization of the excipients and/or the process parameters during spray drying might be needed to improve the nanoparticle characteristics. Furthermore, the LPN powder formulations, spray dried at different weight ratios T/D, display MMADs below 5 μm . Therefore, the produced particles may be suitable for deposition in the lower respiratory tract after pulmonary administration. Moreover, an increase in concentration of dextran as stabilizing excipient during spray drying, provides an increase in the powder flyability. This suggests the importance of the polysaccharide in the stabilization and the aerosol performance of the spray-dried LPN formulations. Finally, an optimization of the PI settings provides a further increase in the flyability of the powder formulations.

Notwithstanding these promising results, further characterization of the formulations is needed to define the optimal ratio of trehalose and dextran as stabilizing excipient, and thereby generate powder particles with aerodynamic and aerosol properties suitable for pulmonary delivery. Cryo-transmission electron microscopy can be used to confirm the structural integrity of the LPNs after spray drying. Furthermore, repetition of the TGA and SEM analysis on the powder formulations, spray dried at all different ratios T/D, is needed to draw a solid conclusion regarding the influence of the residual moisture content and the surface corrugation of the nanocomposite microparticles on the aerosol performance of the powder, respectively. In addition, the particle density of the spray-dried powders could be determined to investigate the impact on the aerosolization properties and to demonstrate the influence of dextran on the powder properties. The measurement of the absolute particle density can be performed by using a gas pycnometer.

After determination of the most promising powder formulation for pulmonary delivery, XRPD can be performed to define either an amorphous or crystalline structure of the obtained powders. This is implemented on the grounds that amorphous structures have better stabilization properties. Moreover, DSC can be used to determine the T_g and melting point of the LPN powder formulation, and to study the influence of stabilizing excipients on the thermodynamic parameters. Finally, the aerosol yield and PSD of the powder can be measured in the PI system to evaluate the suitability of the powder formulations for *in vivo* exposure to the lungs.

Gel electrophoresis with UV visualization can be used to investigate the integrity of siRNA after spray drying of the LPNs. In addition, the *in vitro* siRNA release profiles of the non-spray-dried LPNs and the spray-dried LPNs can be compared to confirm preservation of the quality and the transfection efficiency of the LPNs. Furthermore, the gene silencing activity of the TNF- α siRNA-loaded LPNs should be retained upon reconstitution of the nanocomposite microparticles. The *in vitro* silencing of TNF- α expression can be evaluated at the mRNA level by using the polymerase chain reaction.

7. REFERENCES

1. Okpechi SC, Ghonim MA, Lammi MR. Advances in Chronic Obstructive Pulmonary Disease Therapy: A Vascular-Targeted Approach. *Clinical Medicine Insights: Therapeutics*. 2017;9:1179559X17719127.
2. Barnes PJ. New anti-inflammatory targets for chronic obstructive pulmonary disease. *Nature Reviews Drug Discovery*. 2013;12(7):543-59.
3. Global strategy for the Diagnosis, Management, and Prevention of Chronic Obstructive Pulmonary Disease. Global Initiative for Chronic Obstructive Lung Disease; 2020.
4. Global Health Estimates 2016: Deaths by Cause, Age, Sex, by Country and by Region, 2000-2016. Geneva: World Health Organization; 2018.
5. Halpin DMG, Miravittles M. Chronic Obstructive Pulmonary Disease: The Disease and Its Burden to Society. *Proceedings of the American Thoracic Society*. 2006;3(7):619-23.
6. Pauwels RA, Rabe KF. Burden and clinical features of chronic obstructive pulmonary disease (COPD). *The Lancet*. 2004;364(9434):613-20.
7. Cazzola M, Rogliani P, Ora J, Matera MG. Treatment options for moderate-to-very severe chronic obstructive pulmonary disease. *Expert Opinion on Pharmacotherapy*. 2016;17(7):977-88.
8. Matera MG, Calzetta L, Segreti A, Cazzola M. Emerging drugs for chronic obstructive pulmonary disease. *Expert Opinion on Emerging Drugs*. 2012;17(1):61-82.
9. Cazzola M, Page CP, Calzetta L, Matera MG. Emerging anti-inflammatory strategies for COPD. *European Respiratory Journal*. 2012;40(3):724-41.
10. Jansen MAA, Klausen LH, Thanki K, Lyngsø J, Skov Pedersen J, Franzyk H, et al. Lipidoid-polymer hybrid nanoparticles loaded with TNF siRNA suppress inflammation after intra-articular administration in a murine experimental arthritis model. *European Journal of Pharmaceutics and Biopharmaceutics*. 2019;142:38-48.
11. Fire A, Xu S, Montgomery MK, Kostas SA, Driver SE, Mello CC. Potent and specific genetic interference by double-stranded RNA in *Caenorhabditis elegans*. *Nature*. 1998;391(6669):806-11.
12. Ryther RCC, Flynt AS, Phillips JA, Patton JG. siRNA therapeutics: big potential from small RNAs. *Gene Therapy*. 2005;12(1):5-11.
13. de Fougères A, Vornlocher H-P, Maraganore J, Lieberman J. Interfering with disease: a progress report on siRNA-based therapeutics. *Nature Reviews Drug Discovery*. 2007;6(6):443-53.
14. Elbashir SM, Harborth J, Lendeckel W, Yalcin A, Weber K, Tuschl T. Duplexes of 21-nucleotide RNAs mediate RNA interference in cultured mammalian cells. *Nature*. 2001;411(6836):494-8.
15. A triumph of perseverance over interference. *Nature Biotechnology*. 2018;36(9):775-.
16. Youngren-Ortiz SR, Gandhi NS, España-Serrano L, Chougule MB. Aerosol Delivery of siRNA to the Lungs. Part 1: Rationale for Gene Delivery Systems. *Kona*. 2016;33:63-85.
17. Gavrillov K, Saltzman WM. Therapeutic siRNA: principles, challenges, and strategies. *Yale J Biol Med*. 2012;85(2):187-200.
18. Leung AKK, Tam YYC, Cullis PR. Chapter Four - Lipid Nanoparticles for Short Interfering RNA Delivery. In: Huang L, Liu D, Wagner E, editors. *Advances in Genetics*. 88: Academic Press; 2014. p. 71-110.
19. Miele E, Spinelli GP, Miele E, Di Fabrizio E, Ferretti E, Tomao S, et al. Nanoparticle-based delivery of small interfering RNA: challenges for cancer therapy. *Int J Nanomedicine*. 2012;7:3637-57.
20. Whitehead KA, Langer R, Anderson DG. Knocking down barriers: advances in siRNA delivery. *Nat Rev Drug Discov*. 2009;8(2):129-38.
21. Peer D, Lieberman J. Special delivery: targeted therapy with small RNAs. *Gene Therapy*. 2011;18(12):1127-33.
22. PLGA-Based Nanoparticles as Cancer Drug Delivery Systems. *Asian Pacific Journal of Cancer Prevention*. 2014;15(2):517-35.
23. Ding D, Zhu Q. Recent advances of PLGA micro/nanoparticles for the delivery of biomacromolecular therapeutics. *Materials Science and Engineering: C*. 2018;92:1041-60.

24. Jensen DMK, Cun D, Maltesen MJ, Frokjaer S, Nielsen HM, Foged C. Spray drying of siRNA-containing PLGA nanoparticles intended for inhalation. *Journal of Controlled Release*. 2010;142(1):138-45.
25. Jensen DK, Jensen LB, Koocheki S, Bengtson L, Cun D, Nielsen HM, et al. Design of an inhalable dry powder formulation of DOTAP-modified PLGA nanoparticles loaded with siRNA. *Journal of Controlled Release*. 2012;157(1):141-8.
26. Loney C, Vandenbranden M, Ruyschaert J-M. Cationic lipids activate intracellular signaling pathways. *Advanced Drug Delivery Reviews*. 2012;64(15):1749-58.
27. Hadinoto K, Sundaresan A, Cheow WS. Lipid-polymer hybrid nanoparticles as a new generation therapeutic delivery platform: A review. *European Journal of Pharmaceutics and Biopharmaceutics*. 2013;85(3, Part A):427-43.
28. Thanki K, Zeng X, Justesen S, Tejlmann S, Falkenberg E, Van Driessche E, et al. Engineering of small interfering RNA-loaded lipidoid-poly(DL-lactic-co-glycolic acid) hybrid nanoparticles for highly efficient and safe gene silencing: A quality by design-based approach. *European Journal of Pharmaceutics and Biopharmaceutics*. 2017;120:22-33.
29. Lv H, Zhang S, Wang B, Cui S, Yan J. Toxicity of cationic lipids and cationic polymers in gene delivery. *Journal of Controlled Release*. 2006;114(1):100-9.
30. de Groot AM, Thanki K, Gangloff M, Falkenberg E, Zeng X, van Bijnen DCJ, et al. Immunogenicity Testing of Lipidoids In Vitro and In Silico: Modulating Lipidoid-Mediated TLR4 Activation by Nanoparticle Design. *Mol Ther Nucleic Acids*. 2018;11:159-69.
31. Mukherjee A, Waters AK, Kalyan P, Achrol AS, Kesari S, Yenugonda VM. Lipid-polymer hybrid nanoparticles as a next-generation drug delivery platform: state of the art, emerging technologies, and perspectives. *Int J Nanomedicine*. 2019;14:1937-52.
32. Thanki K, Zeng X, Foged C. Preparation, Characterization, and In Vitro Evaluation of Lipidoid-Polymer Hybrid Nanoparticles for siRNA Delivery to the Cytosol. In: Ogris M, Sami H, editors. *Nanotechnology for Nucleic Acid Delivery: Methods and Protocols*. New York, NY: Springer New York; 2019. p. 141-52.
33. Iqbal M, Zafar N, Fessi H, Elaissari A. Double emulsion solvent evaporation techniques used for drug encapsulation. *International Journal of Pharmaceutics*. 2015;496(2):173-90.
34. Lim YH, Tiemann KM, Hunstad DA, Elsabahy M, Wooley KL. Polymeric nanoparticles in development for treatment of pulmonary infectious diseases. *Wiley Interdiscip Rev Nanomed Nanobiotechnol*. 2016;8(6):842-71.
35. Iyer R, Hsia CCW, Nguyen KT. Nano-Therapeutics for the Lung: State-of-the-Art and Future Perspectives. *Curr Pharm Des*. 2015;21(36):5233-44.
36. De Backer L, Cerrada A, Pérez-Gil J, De Smedt SC, Raemdonck K. Bio-inspired materials in drug delivery: Exploring the role of pulmonary surfactant in siRNA inhalation therapy. *Journal of Controlled Release*. 2015;220:642-50.
37. Thanki K, van Eetvelde D, Geyer A, Fraire J, Hendrix R, Van Eygen H, et al. Mechanistic profiling of the release kinetics of siRNA from lipidoid-polymer hybrid nanoparticles in vitro and in vivo after pulmonary administration. *Journal of Controlled Release*. 2019;310:82-93.
38. Newman SP. Drug delivery to the lungs: challenges and opportunities. *Therapeutic Delivery*. 2017;8(8):647-61.
39. Bustamante-Marin XM, Ostrowski LE. Cilia and Mucociliary Clearance. *Cold Spring Harb Perspect Biol*. 2017;9(4):a028241.
40. Yang W, Peters JI, Williams RO. Inhaled nanoparticles—A current review. *International Journal of Pharmaceutics*. 2008;356(1):239-47.
41. Agu RU, Ugwoke MI, Armand M, Kinget R, Verbeke N. The lung as a route for systemic delivery of therapeutic proteins and peptides. *Respir Res*. 2001;2(4):198-209.
42. Emami F, Vatanara A, Park EJ, Na DH. Drying Technologies for the Stability and Bioavailability of Biopharmaceuticals. *Pharmaceutics*. 2018;10(3):131.

43. Sosnik A, Seremeta KP. Advantages and challenges of the spray-drying technology for the production of pure drug particles and drug-loaded polymeric carriers. *Advances in Colloid and Interface Science*. 2015;223:40-54.
44. Sinsuebpol C, Chatchawalsaisin J, Kulvanich P. Preparation and in vivo absorption evaluation of spray dried powders containing salmon calcitonin loaded chitosan nanoparticles for pulmonary delivery. *Drug Des Devel Ther*. 2013;7:861-73.
45. Fu Y-J, Shyu S-S, Su F-H, Yu P-C. Development of biodegradable co-poly(d,l-lactic/glycolic acid) microspheres for the controlled release of 5-FU by the spray drying method. *Colloids and Surfaces B: Biointerfaces*. 2002;25(4):269-79.
46. Seville PC, Li H-y, Learoyd TP. Spray-Dried Powders for Pulmonary Drug Delivery. 2007;24(4):307-60.
47. Cal K, Sollohub K. Spray Drying Technique. I: Hardware and Process Parameters. *Journal of Pharmaceutical Sciences*. 2010;99(2):575-86.
48. Kanojia G, Willems G-J, Frijlink HW, Kersten GFA, Soema PC, Amorij J-P. A Design of Experiment approach to predict product and process parameters for a spray dried influenza vaccine. *International Journal of Pharmaceutics*. 2016;511(2):1098-111.
49. García GC. Identification of factors of importance for the design and dosing of an inhalable solid dosage form of the tuberculosis subunit vaccine candidate H56/CAF01 [Master's thesis]: University of Copenhagen, Denmark; 2019.
50. Ingvarsson PT, Yang M, Nielsen HM, Rantanen J, Foged C. Stabilization of liposomes during drying. *Expert Opinion on Drug Delivery*. 2011;8(3):375-88.
51. Elsayed I, AbouGhaly MHH. Inhalable nanocomposite microparticles: preparation, characterization and factors affecting formulation. *Expert Opinion on Drug Delivery*. 2016;13(2):207-22.
52. Leekumjorn S, Sum AK. Molecular Dynamics Study on the Stabilization of Dehydrated Lipid Bilayers with Glucose and Trehalose. *The Journal of Physical Chemistry B*. 2008;112(34):10732-40.
53. Wang Y, Beck-Broichsitter M, Yang M, Rantanen J, Bohr A. Investigation of nanocarriers and excipients for preparation of nanoembedded microparticles. *International Journal of Pharmaceutics*. 2017;526(1):300-8.
54. You Y, Zhao M, Liu G, Tang X. Physical characteristics and aerosolization performance of insulin dry powders for inhalation prepared by a spray drying method. *Journal of Pharmacy and Pharmacology*. 2007;59(7):927-34.
55. Tonnis WF, Mensink MA, de Jager A, van der Voort Maarschalk K, Frijlink HW, Hinrichs WLJ. Size and Molecular Flexibility of Sugars Determine the Storage Stability of Freeze-Dried Proteins. *Molecular Pharmaceutics*. 2015;12(3):684-94.
56. Chang L, Shepherd D, Sun J, Ouellette D, Grant KL, Tang X, et al. Mechanism of protein stabilization by sugars during freeze-drying and storage: Native structure preservation, specific interaction, and/or immobilization in a glassy matrix? *Journal of Pharmaceutical Sciences*. 2005;94(7):1427-44.
57. Mensink MA, Frijlink HW, van der Voort Maarschalk K, Hinrichs WLJ. How sugars protect proteins in the solid state and during drying (review): Mechanisms of stabilization in relation to stress conditions. *European Journal of Pharmaceutics and Biopharmaceutics*. 2017;114:288-95.
58. Grasmeijer N, Stankovic M, de Waard H, Frijlink HW, Hinrichs WLJ. Unraveling protein stabilization mechanisms: Vitrification and water replacement in a glass transition temperature controlled system. *Biochimica et Biophysica Acta (BBA) - Proteins and Proteomics*. 2013;1834(4):763-9.
59. Crowe JH, Carpenter JF, Crowe LM. THE ROLE OF VITRIFICATION IN ANHYDROBIOSIS. *Annual Review of Physiology*. 1998;60(1):73-103.
60. Jain NK, Roy I. Effect of trehalose on protein structure. *Protein Sci*. 2009;18(1):24-36.
61. Hinrichs WLJ, Sanders NN, De Smedt SC, Demeester J, Frijlink HW. Inulin is a promising cryo- and lyoprotectant for PEGylated lipoplexes. *Journal of Controlled Release*. 2005;103(2):465-79.

62. Allison SD, Manning MC, Randolph TW, Middleton K, Davis A, Carpenter JF. Optimization of storage stability of lyophilized actin using combinations of disaccharides and dextran. *Journal of Pharmaceutical Sciences*. 2000;89(2):199-214.
63. Chapter 7 - Preparations for inhalation. *European Pharmacopeia 10.0 ed*. Strasbourg, France: European Directorate for Quality in Medicines and Healthcare (EDQM); 2020.
64. Dolovich MB, Dhand R. Aerosol drug delivery: developments in device design and clinical use. *The Lancet*. 2011;377(9770):1032-45.
65. Kaplan A, Price D. Matching Inhaler Devices with Patients: The Role of the Primary Care Physician. *Can Respir J*. 2018;2018:9473051-
66. Leng D, Thanki K, Foged C, Yang M. Formulating Inhalable Dry Powders Using Two-Fluid and Three-Fluid Nozzle Spray Drying. *Pharmaceutical Research*. 2018;35(12):247.
67. Zhou Q, Tang P, Leung SSY, Chan JGY, Chan H-K. Emerging inhalation aerosol devices and strategies: Where are we headed? *Advanced Drug Delivery Reviews*. 2014;75:3-17.
68. Zhou Q, Leung SSY, Tang P, Parumasivam T, Loh ZH, Chan H-K. Inhaled formulations and pulmonary drug delivery systems for respiratory infections. *Advanced Drug Delivery Reviews*. 2015;85:83-99.
69. Momin MAM, Rangnekar B, Sinha S, Cheung C-Y, Cook GM, Das SC. Inhalable Dry Powder of Bedaquiline for Pulmonary Tuberculosis: In Vitro Physicochemical Characterization, Antimicrobial Activity and Safety Studies. *Pharmaceutics*. 2019;11(10):502.
70. Yildiz-Peköz A, Akbal O, Tekarslan SH, Sagirli AO, Mulazimoglu L, Morina D, et al. Preparation and Characterization of Doripenem-Loaded Microparticles for Pulmonary Delivery. *Journal of Aerosol Medicine and Pulmonary Drug Delivery*. 2018;31(6):347-57.
71. Mitchell J, Newman S, Chan H-K. In vitro and in vivo aspects of cascade impactor tests and inhaler performance: a review. *AAPS PharmSciTech*. 2007;8(4):E110-E.
72. Section 2.9.18 - Preparation for inhalation: aerodynamic assessment for fine particles. *European Pharmacopeia 10.0 ed*. Strasbourg, France: European Directorate for Quality in Medicines and Healthcare (EDQM); 2020. p. 347- 60.
73. Roberts DL, Mitchell JP. Measurement of Aerodynamic Particle Size Distribution of Orally Inhaled Products by Cascade Impactor: How to Let the Product Specification Drive the Quality Requirements of the Cascade Impactor. *AAPS PharmSciTech*. 2019;20(2):57.
74. Fioni A, Selg E, Cenacchi V, Acevedo F, Brogin G, Gerde P, et al. Investigation of Lung Pharmacokinetic of the Novel PDE4 Inhibitor CHF6001 in Preclinical Models: Evaluation of the PreciseInhale Technology. *Journal of Aerosol Medicine and Pulmonary Drug Delivery*. 2017;31(1):61-70.
75. The power of precision. Huddinge, Sweden: Inhalation sciences; [25/04/2020]. white paper]. Available from: <http://inhalation.se/products/white-paper/>.
76. Selg E, Ewing P, Acevedo F, Sjöberg C-O, Ryrfeldt Å, Gerde P. Dry Powder Inhalation Exposures of the Endotracheally Intubated Rat Lung, Ex Vivo and In Vivo: The Pulmonary Pharmacokinetics of Fluticasone Furoate. *Journal of Aerosol Medicine and Pulmonary Drug Delivery*. 2012;26(4):181-9.
77. Malmlöf M, Nowenwik M, Meelich K, Rådberg I, Selg E, Burns J, et al. Effect of particle deposition density of dry powders on the results produced by an in vitro test system simulating dissolution- and absorption rates in the lungs. *European Journal of Pharmaceutics and Biopharmaceutics*. 2019;139:213-23.
78. Lexmond AJ, Keir S, Terakosolphan W, Page CP, Forbes B. A novel method for studying airway hyperresponsiveness in allergic guinea pigs in vivo using the PreciseInhale system for delivery of dry powder aerosols. *Drug Deliv Transl Res*. 2018;8(3):760-9.
79. Selg E, Acevedo F, Nybom R, Blomgren B, Ryrfeldt Å, Gerde P. Delivering Horseradish Peroxidase as a Respirable Powder to the Isolated, Perfused, and Ventilated Lung of the Rat: The Pulmonary Disposition of an Inhaled Model Biopharmaceutical. *Journal of Aerosol Medicine and Pulmonary Drug Delivery*. 2010;23(5):273-84.

80. Ji J, Upadhyay S, Xiong X, Malmlöf M, Sandström T, Gerde P, et al. Multi-cellular human bronchial models exposed to diesel exhaust particles: assessment of inflammation, oxidative stress and macrophage polarization. *Part Fibre Toxicol.* 2018;15(1):19-.
81. Cappellini F, Di Bucchianico S, Karri V, Latvala S, Malmlöf M, Kippler M, et al. Dry Generation of CeO₂ Nanoparticles and Deposition onto a Co-Culture of A549 and THP-1 Cells in Air-Liquid Interface—Dosimetry Considerations and Comparison to Submerged Exposure. *Nanomaterials.* 2020;10(4):618.
82. Dormenval C, Lokras A, Cano-Garcia G, Wadhwa A, Thanki K, Rose F, et al. Identification of Factors of Importance for Spray Drying of Small Interfering RNA-Loaded Lipidoid-Polymer Hybrid Nanoparticles for Inhalation. *Pharmaceutical Research.* 2019;36(10):142.
83. Gerde P, Ewing P, Låstbom L, Ryrfeldt Å, Waher J, Lidén G. A Novel Method to Aerosolize Powder for Short Inhalation Exposures at High Concentrations: Isolated Rat Lungs Exposed to Respirable Diesel Soot. *Inhalation Toxicology.* 2004;16(1):45-52.
84. Dormenval C. Identification of factors of importance for the design of an inhalable solid dosage form of small interfering RNA-loaded lipidoid-poly(DL-lactic-co-glycolic acid) hybrid nanoparticles [Master's thesis]: University of Copenhagen, Denmark; 2018.
85. Ingvarsson PT, Yang M, Mulvad H, Nielsen HM, Rantanen J, Foged C. Engineering of an Inhalable DDA/TDB Liposomal Adjuvant: A Quality-by-Design Approach Towards Optimization of the Spray Drying Process. *Pharmaceutical Research.* 2013;30(11):2772-84.
86. Maltesen MJ, Bjerregaard S, Hovgaard L, Havelund S, van de Weert M. Quality by design – Spray drying of insulin intended for inhalation. *European Journal of Pharmaceutics and Biopharmaceutics.* 2008;70(3):828-38.
87. Yang F, Liu X, Wang W, Liu C, Quan L, Liao Y. The effects of surface morphology on the aerosol performance of spray-dried particles within HFA 134a based metered dose formulations. *Asian Journal of Pharmaceutical Sciences.* 2015;10(6):513-9.
88. Chew NYK, Tang P, Chan H-K, Raper JA. How Much Particle Surface Corrugation Is Sufficient to Improve Aerosol Performance of Powders? *Pharmaceutical Research.* 2005;22(1):148-52.
89. Chew NYK, Chan H-K. Use of Solid Corrugated Particles to Enhance Powder Aerosol Performance. *Pharmaceutical Research.* 2001;18(11):1570-7.
90. Murugappan S, Patil HP, Kanojia G, ter Veer W, Meijerhof T, Frijlink HW, et al. Physical and immunogenic stability of spray freeze-dried influenza vaccine powder for pulmonary delivery: Comparison of inulin, dextran, or a mixture of dextran and trehalose as protectants. *European Journal of Pharmaceutics and Biopharmaceutics.* 2013;85(3, Part A):716-25.
91. Elversson J, Millqvist-Fureby A. Particle Size and Density in Spray Drying—Effects of Carbohydrate Properties. *Journal of Pharmaceutical Sciences.* 2005;94(9):2049-60.
92. Ingvarsson PT, Schmidt ST, Christensen D, Larsen NB, Hinrichs WLJ, Andersen P, et al. Designing CAF-adjuvanted dry powder vaccines: Spray drying preserves the adjuvant activity of CAF01. *Journal of Controlled Release.* 2013;167(3):256-64.

